arXiv:0801.1796v2 [hep-ph] 3 Apr 2008

Preprint typeset in JHEP style - HYPER VERSION

Light-cone sum rules for $B \to \pi$ form factors revisited

G. Duplančić*

Max-Planck-Institut fur Physik (Werner-Heisenberg-Institut), Föhringer Ring 6, D-80805 München, Germany
Rudjer Boskovic Institute, Theoretical Physics Division, HR-10002 Zagreb, Croatia
E-mail: gorand@thphys.irb.hr

A. Khodjamirian

Theoretische Physik 1, Fachbereich Physik, Universität Siegen, D-57068 Siegen, Germany
E-mail: khodjam@hep.physik.uni-siegen.de

Th. Mannel

Theoretische Physik 1, Fachbereich Physik, Universität Siegen, D-57068 Siegen, Germany
E-mail: mannel@hep.physik.uni-siegen.de

B. Melić

Rudjer Boskovic Institute, Theoretical Physics Division, HR-10002 Zagreb, Croatia
E-mail: melic@thphys.irb.hr

N. Offen

Laboratoire de Physique Théorique CNRS/Univ. Paris-Sud 11, F-91405 Orsay, France
E-mail: nils.offen@th.u-psud.fr

Abstract: We reconsider and update the QCD light-cone sum rules for $B \to \pi$ form factors. The gluon radiative corrections to the twist-2 and twist-3 terms in the correlation functions are calculated. The $\overline{MS}$ b-quark mass is employed, instead of the one-loop pole mass used in the previous analyses. The light-cone sum rule for $f^+_{B\pi}(q^2)$ is fitted to the measured q^2-distribution in $B \to \pi l \nu_l$, fixing the input parameters with the largest uncertainty: the Gegenbauer moments of the pion distribution amplitude. For the $B \to \pi$ vector form factor at zero momentum transfer we predict $f^+_{B\pi}(0) = 0.26^{+0.04}_{-0.03}$. Combining it with the value of the product $|V_{ub} f^+_{B\pi}(0)|$ extracted from experiment, we obtain $|V_{ub}| = (3.5 \pm 0.4 \pm 0.2 \pm 0.1) \times 10^{-3}$. In addition, the scalar and penguin $B \to \pi$ form factors $f^0_{B\pi}(q^2)$ and $f^T_{B\pi}(q^2)$ are calculated.

Keywords: B-decays, QCD, Sum rules.

*Alexander von Humboldt Fellow

Contents

1. Introduction

The form factors of heavy-to-light transitions at large energies of the final hadrons are among the most important applications of QCD light-cone sum rules (LCSR) [1]. In this paper we concentrate on the $B \to \pi$ transition form factors $f^+_{B\pi}$, $f^0_{B\pi}$ and $f^T_{B\pi}$ of the electroweak vector $b \to u$ and penguin $b \to d$ currents, respectively. Previously, these form factors have been calculated from LCSR in [2, 3, 4, 5, 6, 7, 8, 9, 10], gradually improving the accuracy.

The main advantage of LCSR is the possibility to perform calculations in full QCD, with a finite b-quark mass. In the sum rule approach, the $B \to \pi$ matrix element is obtained from the correlation function of quark currents, rather than estimated directly from a certain factorization ansatz. This correlation function is conveniently "designed", so that, at large spacelike external momenta, the operator-product expansion (OPE) near the light-cone is applicable. Within OPE, the correlation function is factorized in a series of hard-scattering amplitudes convoluted with the pion light-cone distribution amplitudes (DA's) of growing twist. To obtain the $B \to \pi$ form factors from the correlation function, one makes use of the hadronic dispersion relation and quark-hadron duality in the B-meson channel, following the general strategy of QCD sum rules [11]. More details can be found in the reviews on LCSR, e.g., in [12, 13, 14]. A modification of the method, involving B-meson distribution amplitudes and dispersion relation in the pion channel was recently suggested in [15]; the analogous sum rules for $B \to \pi$ form factors in soft-collinear effective theory (SCET) were derived in [16].

LCSR provide analytic expressions for the form factors, including both hard-scattering and soft (end-point) contributions. Because the method is based on a calculation in full QCD, combined with a rigorous hadronic dispersion relation, the uncertainties in the resulting LCSR are identifiable and assessable. These uncertainties are caused by the truncation of the light-cone OPE, and by the limited accuracy of the universal input, such as the quark masses and parameters of the pion DA's. In addition, a sort of systematic uncertainty is brought by the quark-hadron duality approximation adopted for the contribution of excited hadronic states in the dispersion relation. Importantly, $B \to \pi$ form factors are calculable from LCSR in the region of small momentum transfer q^2 (large energy of the pion), not yet directly accessible to lattice QCD.

The $B \to \pi l \nu_l$ decays, with continuously improving experimental data, provide nowadays the most reliable exclusive V_{ub} determination. Along with the lattice QCD results, the form factor $f^+_{B\pi}(q^2)$ obtained [10] from LCSR is used for the $|V_{ub}|$ extraction. Furthermore, the LCSR form factors $f^{+,0}_{B\pi}(q^2)$ can provide inputs for various factorization approaches to exclusive B decays, such as QCD factorization [17], whereas the penguin form factor $f^T_{B\pi}$ is necessary for the analysis of the rare $B \to \pi l^+ l^-$ decay. Having in mind the importance of $B \to \pi$ form factors for the V_{ub} determination and for the phenomenological analysis of various exclusive B decays, we decided to reanalyze and update the LCSR for these form factors. One of our motivations was to recalculate the $O(\alpha_s)$ gluon radiative correction to the twist-3 part of the correlation function. Only a single calculation of this term exists [9, 10], whereas the $O(\alpha_s)$ corrections to the twist-2 part have been independently obtained in [4] and [5]. In what follows, we derive and present the explicit expressions for all $O(\alpha_s)$ hard-scattering amplitudes and their imaginary parts for the twist-2 and twist-3 parts of the correlation function and some of these expressions are new.

In the OPE of the correlation function the $\overline{MS}$ mass $\overline{m}_b(\mu)$ is used, a natural choice for a virtual b-quark propagating in the hard-scattering amplitudes, calculated at large spacelike momentum scales $\sim m_b$. Importantly, in the resulting sum rules we keep using the $\overline{MS}$ mass. Note that the value of $\overline{m}_b(\overline{m}_b)$ is rather accurately determined from the bottomonium sum rules. In previous analyses, the one-loop pole mass of the b-quark was employed in LCSR. The main motivation was that the pole mass was used also in the two-point sum rule for the B-meson decay constant f_B, needed to extract the form factor from LCSR. In the meantime, the f_B sum rule is available also in $\overline{MS}$-scheme [18], and we apply this new version here.

Furthermore, we fix the most uncertain input parameters, the effective threshold and simultaneously, the Gegenbauer moments of the pion twist-2 DA, by calculating the B-meson mass and the shape of $f^+_{B\pi}(q^2)$ from LCSR and fitting these quantities to their measured values. In addition, the nonperturbative parameters of the twist-3,4 pion DA's entering LCSR are updated, using the results of the recent analysis [19].

The paper is organized as follows. In sect. 2 the correlation function is introduced and the leading-order (LO) terms of OPE are presented, including the contributions of the pion twist-2,3,4 two-particle DA's and twist-3,4 three-particle DA's. In sect. 3 the calculation of the $O(\alpha_s)$ twist-2 and twist-3 parts of the correlation function is discussed. In sect. 4 we present LCSR for all three $B \to \pi$ form factors. Sect. 5 contains the discussion of the numerical input and results, as well as the estimation of theoretical uncertainties, and finally, the determination of $|V_{ub}|$. Sect. 6 is devoted to the concluding discussion. App. A contains the necessary formulae and input for the pion DA's. The bulky expressions for the $O(\alpha_s)$ hard-scattering amplitudes and their imaginary parts are collected in App. B, and the sum rule for f_B is given in App. C.

2. Correlation function

The vacuum-to-pion correlation function used to obtain the LCSR for the form factors of $B \to \pi$ transitions is defined as:

$$
\begin{aligned}
F_\mu(p,q) &= i \int d^4x\, e^{iq\cdot x} \langle \pi^+(p)| T\left\{\bar{u}(x)\Gamma_\mu b(x), m_b \bar{b}(0) i\gamma_5 d(0)\right\}|0\rangle \\
&= \begin{cases} F(q^2,(p+q)^2)p_\mu + \widetilde{F}(q^2,(p+q)^2)q_\mu\,, & \Gamma_\mu = \gamma_\mu \\[2ex] F^T(q^2,(p+q)^2)\left[p_\mu q^2 - q_\mu(qp)\right], & \Gamma_\mu = -i\sigma_{\mu\nu}q^\nu \end{cases}
\end{aligned}
\tag{2.1}
$$

for the two different $b \to u$ transition currents, For definiteness, we consider the $\bar{B}_d \to \pi^+$ flavour configuration and, for simplicity we use u instead of d in the penguin current, which does not make difference in the adopted isospin symmetry limit. Working in the chiral limit, we neglect the pion mass ($p^2 = m_\pi^2 = 0$) and the u-, d-quark masses, whereas the ratio $\mu_\pi = m_\pi^2/(m_u + m_d)$ remains finite.

At $q^2 \ll m_b^2$ and $(p+q)^2 \ll m_b^2$, that is, far from the b-flavour thresholds, the b quark propagating in the correlation function is highly virtual and the distances near the light-cone $x^2 = 0$ dominate. It is possible to prove the light-cone dominance, following the same line of arguments as in [15]. Contracting the b-quark fields, one expands the vacuum-to pion matrix element in terms of the pion light-cone DA's of growing twist. The light-cone expansion [20] of the b-quark propagator is used (see also [3]):

$$
\begin{aligned}
\langle 0|b^i_\alpha(x)\bar{b}^j_\beta(0)|0\rangle = -i\int \frac{d^4k}{(2\pi)^4}e^{-ik\cdot x}\Bigg[\delta^{ij}\frac{\not{k}+m}{m^2-k^2} \\
+g_s\int\limits_0^1 dv G^{\mu\nu a}(vx)\left(\frac{\lambda^a}{2}\right)^{ij}\left(\frac{\not{k}+m}{2(m^2-k^2)^2}\sigma_{\mu\nu} + \frac{1}{m^2-k^2}vx_\mu\gamma_\nu\right)\Bigg]_{\alpha\beta}\,,
\end{aligned}
\tag{2.2}
$$

where only the free propagator and the one-gluon term are retained. The latter term gives rise to the three-particle DA's in the OPE. Diagrammatically, the contributions of two- and three-particle DA's to the correlation function are depicted in Fig. 1. In terms of perturbative QCD, these are LO (zeroth order in α_s) contributions. The Fock components of the pion with multiplicities larger than three, are neglected, as well as the twists higher

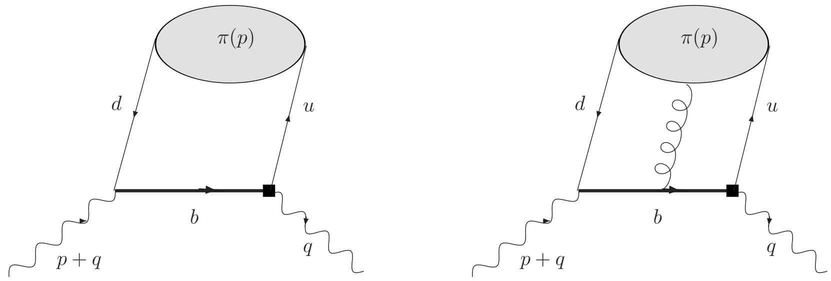

Figure 1: *Diagrams representing the leading-order terms in the correlation function involving the two-particle (left) and three-particle (right) pion DA's shown by ovals. Solid, curly and wave lines represent quarks, gluons, and external currents, respectively.*

than 4. This truncation is justified by the fact that the twist-4 and three-particle corrections to LCSR obtained below turn out to be very small.

In addition we include the $O(\alpha_s)$ gluon radiative corrections to the dominant twist-2 and twist-3 parts of the correlation function. The OPE result for the invariant amplitude F is then represented as a sum of LO and NLO parts:

$$F(q^2,(p+q)^2) = F_0(q^2,(p+q)^2) + \frac{\alpha_s C_F}{4\pi} F_1(q^2,(p+q)^2), \tag{2.3}$$

and the same for $\widetilde{F}$ and F^T. The leading-order (LO) invariant amplitudes F_0, $\widetilde{F}_0$, and F_0^T including twist 2,3,4 contributions have been obtained earlier in [3, 6, 7, 21]. We present them here switching to the new notations [19] of the twist-3,4 DA's:

$$\begin{aligned} F_0(q^2,(p+q)^2) = m_b^2 f_\pi \int\limits_0^1 \frac{du}{m_b^2-(q+up)^2}\Bigg\{ \varphi_\pi(u) + \frac{\mu_\pi}{m_b} u \phi_{3\pi}^p(u) \\ + \frac{\mu_\pi}{6m_b}\left[2 + \frac{m_b^2+q^2}{m_b^2-(q+up)^2}\right]\phi_{3\pi}^\sigma(u) - \frac{m_b^2\phi_{4\pi}(u)}{2\big(m_b^2-(q+up)^2\big)^2} \\ - \frac{u}{m_b^2-(q+up)^2}\int\limits_0^u dv \psi_{4\pi}(v)\Bigg\} \\ + \int\limits_0^1 dv \int \frac{\mathcal{D}\alpha}{\big[m_b^2-\big(q+(\alpha_1+\alpha_3 v)p\big)^2\big]^2}\Bigg\{ 4m_b f_{3\pi} v (q\cdot p)\Phi_{3\pi}(\alpha_i) \\ + m_b^2 f_\pi \Big(2\Psi_{4\pi}(\alpha_i) - \Phi_{4\pi}(\alpha_i) + 2\widetilde{\Psi}_{4\pi}(\alpha_i) - \widetilde{\Phi}_{4\pi}(\alpha_i)\Big)\Bigg\}, \end{aligned} \tag{2.4}$$

$$\widetilde{F}_0(q^2,(p+q)^2) = m_b f_\pi \int\limits_0^1 \frac{du}{m_b^2-(q+up)^2}\Bigg\{\mu_\pi \phi^p_{3\pi}(u) + \frac{\mu_\pi}{6}\left[1-\frac{m_b^2-q^2}{m_b^2-(q+up)^2}\right]\frac{\phi^\sigma_{3\pi}(u)}{u} - \frac{m_b}{m_b^2-(q+up)^2}\int\limits_0^u dv\psi_{4\pi}(v)\Bigg\}, \tag{2.5}$$

$$F_0^T(q^2,(p+q)^2) = m_b f_\pi \int\limits_0^1 \frac{du}{m_b^2-(q+up)^2}\Bigg\{\varphi_\pi(u) + \frac{m_b\mu_\pi}{3(m_b^2-(q+up)^2)}\phi^\sigma_{3\pi}(u) - \frac{1}{2(m_b^2-(q+up)^2)}\left(\frac{1}{2}+\frac{m_b^2}{m_b^2-(q+up)^2}\right)\phi_{4\pi}(u)\Bigg\}$$
$$+m_b f_\pi \int\limits_0^1 dv \int \frac{\mathcal{D}\alpha}{\left[m_b^2-\left(q+(\alpha_1+\alpha_3 v)p\right)^2\right]^2}\Bigg\{2\Psi_{4\pi}(\alpha_i)-(1-2v)\Phi_{4\pi}(\alpha_i) +2(1-2v)\widetilde{\Psi}_{4\pi}(\alpha_i)-\widetilde{\Phi}_{4\pi}(\alpha_i)\Bigg\}, \tag{2.6}$$

where $\mathcal{D}\alpha = d\alpha_1 d\alpha_2 d\alpha_3 \delta(1-\alpha_1-\alpha_2-\alpha_3)$, and the definitions of the twist-2 (φ_π), twist-3 ($\phi^p_{3\pi}$, $\phi^\sigma_{3\pi}$, $\Phi_{3\pi}$) and twist-4 ($\phi_{4\pi}$, $\psi_{4\pi}$, $\Phi_{4\pi}$, $\Psi_{4\pi}$, $\widetilde{\Phi}_{4\pi}$, $\widetilde{\Psi}_{4\pi}$) pion DA's and their parameters are presented in App. A. Note that all twist-4 terms are suppressed with respect to leading twist-2 terms, with an additional power of the denominator $1/(m_b^2-(q+up)^2)$ compensated by the normalization parameter $\delta_\pi^2 \sim \Lambda_{QCD}^2$ of the twist-4 DA's.

The calculation of the NLO amplitudes $F_1, \tilde{F}_1, F_1^T$ will be discussed in the next section.

3. Gluon radiative corrections

In the light-cone OPE of the correlation function (2.1) each twist component receives gluon radiative corrections. To obtain the desired NLO terms, one has to calculate the $O(\alpha_s)$ one-loop diagrams shown in Fig. 2, convoluting them with the twist-2 and two-particle twist-3 DA's, respectively. The diagrams are computed using the standard dimensional regularization and $\overline{MS}$ scheme. In addition, in our calculation the reduction method from [22] is employed.

The invariant amplitude F_1 in (2.3) is obtained in a factorized form of the convolutions:

$$F_1(q^2,(p+q)^2) = f_\pi \int_0^1 du \Bigg\{T_1(q^2,(p+q)^2,u)\varphi_\pi(u) + \frac{\mu_\pi}{m_b}\left[T_1^p(q^2,(p+q)^2,u)\phi^p_{3\pi}(u) + T_1^\sigma(q^2,(p+q)^2,u)\phi^\sigma_{3\pi}(u)\right]\Bigg\}, \tag{3.1}$$

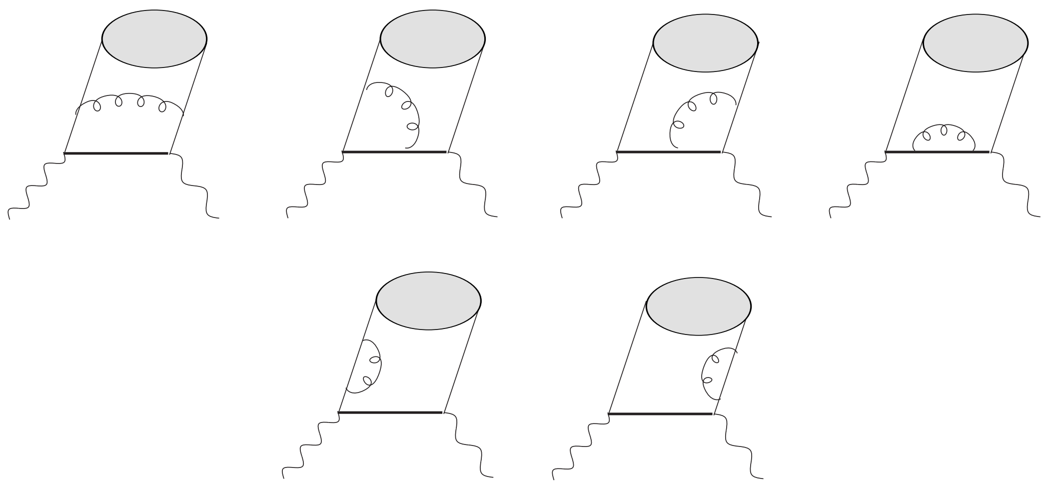

Figure 2: *Diagrams corresponding to the $O(\alpha_s)$ gluon radiative corrections to the correlation function.*

where the hard-scattering amplitudes T_1, $T_1^{p,\sigma}$ result from the calculation of the diagrams in Fig.2. The two other NLO amplitudes $\widetilde{F}_1$ and $m_b F_1^T$ have the same expressions with $T_1 \to \widetilde{T}_1$, $T_1^{p,\sigma} \to \widetilde{T}_1^{p,\sigma}$, and $T_1 \to T_1^T$, $T_1 \to T_1^{Tp,\sigma}$, respectively. The resulting expressions for all hard-scattering amplitudes are presented in App. B. Note that the LO expressions for the correlation functions in (2.4)-(2.6) also have a factorized, albeit a much simpler form, with the zeroth-order in α_s hard-scattering amplitudes stemming from the free propagator of the virtual b-quark. In particular, the twist-2 component in F_0 is a convolution of $T_0 = m_b^2/[m_b^2 - (q+up)^2]$ with $\varphi_\pi(u)$.

Let us mention some important features of the $O(\alpha_s)$ terms of OPE. The currents $\bar{u}\gamma_\mu b$ and $m_b \bar{b} i\gamma_5 d$ in the correlation function are physical and not renormalizable. Hence, the ultraviolet singularities appearing in T_1 and $\widetilde{T}_1$ are canceled by the renormalization of the heavy quark mass. For T_1^T an additional renormalization of the composite $\overline{q}\sigma_{\mu\nu}b$ operator has to be taken into account. Furthermore, in the twist-2 term in (3.1) the convolution integral is convergent due to collinear factorization. As explicitly shown in [4, 5], the infrared-collinear divergences of the $O(\alpha_s)$ diagrams are absorbed by the well known one-loop evolution [23] of the twist-2 pion DA. As a result of factorization, a residual dependence on the factorization scale μ_f enters the amplitude T_1 and the twist-2 DA φ_π. This scale effectively separates the long- and short (near the light-cone) distances in the correlation function. In the twist-3 part of F_1, the complete evolution kernel has to include the mixing of two- and three-particle DA's. To avoid these complications, and following [9], the twist-3 pion DA's in (3.1) are taken in their asymptotic form: $\phi_p(u) = 1$ and $\phi_\sigma(u) = 6u(1-u)$, whereas the nonasymptotic effects in these DA's are only included in the LO part F_0. We checked that the infrared divergences appearing in the amplitudes T_1^p and T_1^σ cancel in the sum of the ϕ_p and ϕ_σ contributions with the one-loop renormalization of the parameter μ_π (i.e., of the quark condensate density). Finally, in accordance with [9, 10], all renormalized hard-scattering amplitudes are well behaved at the end-points $u = 0, 1$, regardless of the form of the DA's.

After completing the calculation of OPE terms with the LO (NLO) accuracy up to twist-4 (twist-3), we turn now to the derivation of the sum rules.

4. LCSR for $B \to \pi$ form factors

In the LCSR approach the $B \to \pi$ matrix elements are related to the correlation function (2.1) via hadronic dispersion relation in the channel of the $\bar{b}\gamma_5 d$ current with the four-momentum squared $(p+q)^2$. Inserting hadronic states between the currents in (2.1) one isolates the ground-state B-meson contributions in the dispersion relations for all three invariant amplitudes:

$$\begin{aligned} F(q^2,(p+q)^2) &= \frac{2m_B^2 f_B f^+_{B\pi}(q^2)}{m_B^2-(p+q)^2} + \dots \\ \widetilde{F}(q^2,(p+q)^2) &= \frac{m_B^2 f_B [f^+_{B\pi}(q^2)+f^-_{B\pi}(q^2)]}{m_B^2-(p+q)^2} + \dots \\ F^T(q^2,(p+q)^2) &= \frac{2m_B^2 f_B f^T_{B\pi}(q^2)}{(m_B+m_\pi)(m_B^2-(p+q)^2)} + \dots \end{aligned} \tag{4.1}$$

where the ellipses indicate the contributions of heavier states (starting from $B^*\pi$). The three $B \to \pi$ form factors entering the residues of the B pole in (4.1) are defined as:

$$\langle \pi^+(p)|\bar{u}\gamma_\mu b|\bar{B}_d(p+q)\rangle = 2f^+_{B\pi}(q^2)p_\mu + \left(f^+_{B\pi}(q^2)+f^-_{B\pi}(q^2)\right) q_\mu\,, \tag{4.2}$$

$$\langle \pi^+(p)|\bar{u}\sigma_{\mu\nu}q^\nu b|\bar{B}_d(p+q)\rangle = \Big[q^2(2p_\mu+q_\mu)-(m_B^2-m_\pi^2)q_\mu\Big]\frac{i f^T_{B\pi}(q^2)}{m_B+m_\pi}\,, \tag{4.3}$$

and $f_B = \langle \bar{B}_d|m_b\bar{b}i\gamma_5 d|0\rangle/m_B^2$ is the B-meson decay constant.

Substituting the OPE results for F, $\widetilde{F}$ and F^T in l.h.s. of (4.1), one approximates the contributions of the heavier states in r.h.s. with the help of quark-hadron duality, introducing the effective threshold parameter s_0^B. After the Borel transformation in the variable $(p+q)^2 \to M^2$, the sum rules for all three $B \to \pi$ form factors are obtained. The LCSR for the vector form factor reads:

$$f^+_{B\pi}(q^2) = \frac{e^{m_B^2/M^2}}{2m_B^2 f_B}\left[F_0(q^2,M^2,s_0^B) + \frac{\alpha_s C_F}{4\pi}F_1(q^2,M^2,s_0^B)\right], \tag{4.4}$$

where $F_{0(1)}(q^2,M^2,s_0^B)$ originates from the OPE result for the LO (NLO) invariant amplitude $F_{0(1)}(q^2,(p+q)^2)$.

The LO part of the LCSR has the following expression:

$$\begin{aligned} F_0(q^2,M^2,s_0^B) &= m_b^2 f_\pi \int\limits_{u_0}^{1} du\, e^{-\frac{m_b^2-q^2\bar{u}}{uM^2}} \Bigg\{ \frac{\varphi_\pi(u)}{u} \\ &+ \frac{\mu_\pi}{m_b}\left(\phi^p_{3\pi}(u) + \frac{1}{6}\left[\frac{2\phi^\sigma_{3\pi}(u)}{u} - \left(\frac{m_b^2+q^2}{m_b^2-q^2}\right)\frac{d\phi^\sigma_{3\pi}(u)}{du}\right]\right) - 2\left(\frac{f_{3\pi}}{m_b f_\pi}\right)\frac{I_{3\pi}(u)}{u} \\ &+ \frac{1}{m_b^2-q^2}\left(-\frac{m_b^2 u}{4(m_b^2-q^2)}\frac{d^2\phi_{4\pi}(u)}{du^2} + u\psi_{4\pi}(u) + \int\limits_0^u dv\psi_{4\pi}(v) - I_{4\pi}(u)\right)\Bigg\}, \end{aligned} \tag{4.5}$$

where $\bar{u} = 1 - u$, $u_0 = (m_b^2 - q^2)/(s_0^B - q^2)$ and the short-hand notations introduced for the integrals over three-particle DA's are:

$$I_{3\pi}(u) = \frac{d}{du}\left(\int\limits_0^u d\alpha_1 \int\limits_{(u-\alpha_1)/(1-\alpha_1)}^1 dv\ \Phi_{3\pi}(\alpha_i)\Bigg|_{\substack{\alpha_2 = 1-\alpha_1-\alpha_3,\\ \alpha_3 = (u-\alpha_1)/v}}\right),$$

$$I_{4\pi}(u) = \frac{d}{du}\left(\int\limits_0^u d\alpha_1 \int\limits_{(u-\alpha_1)/(1-\alpha_1)}^1 \frac{dv}{v}\Big[2\Psi_{4\pi}(\alpha_i) - \Phi_{4\pi}(\alpha_i) + 2\widetilde{\Psi}_{4\pi}(\alpha_i) - \widetilde{\Phi}_{4\pi}(\alpha_i)\Big]\Bigg|_{\substack{\alpha_2 = 1-\alpha_1-\alpha_3,\\ \alpha_3 = (u-\alpha_1)/v}}\right). \quad (4.6)$$

The NLO term in (4.4) is cast in the form of the dispersion relation:

$$F_1(q^2, M^2, s_0^B) = \frac{1}{\pi}\int\limits_{m_b^2}^{s_0^B} ds e^{-s/M^2}\, \mathrm{Im}_s F_1(q^2, s)$$
$$= \frac{f_\pi}{\pi}\int\limits_{m_b^2}^{s_0^B} ds e^{-s/M^2}\int_0^1 du\Big\{\mathrm{Im}_s T_1(q^2, s, u)\,\varphi_\pi(u)$$
$$+\frac{\mu_\pi}{m_b}\Big[\mathrm{Im}_s T_1^p(q^2, s, u)\,\phi_{3\pi}^p(u) + \mathrm{Im}_s T_1^\sigma(q^2, s, u)\,\phi_{3\pi}^\sigma(u)\Big]\Big\}, \quad (4.7)$$

where the bulky expressions for the imaginary parts of the amplitudes T_1,T_1^p,T_1^σ are presented in App. B.

The LCSR following from the dispersion relation for the invariant amplitude $\widetilde{F}$ in (4.1) reads:

$$f_{B\pi}^+(q^2) + f_{B\pi}^-(q^2) = \frac{e^{m_B^2/M^2}}{m_B^2 f_B}\left[\widetilde{F}_0(q^2, M^2, s_0^B) + \frac{\alpha_s C_F}{4\pi}\widetilde{F}_1(q^2, M^2, s_0^B)\right], \quad (4.8)$$

where

$$\widetilde{F}_0(q^2, M^2, s_0^B) = m_b^2 f_\pi \int\limits_{u_0}^1 du\, e^{-\frac{m_b^2 - q^2\bar{u}}{uM^2}}\left\{\frac{\mu_\pi}{m_b}\left(\frac{\phi_{3\pi}^p(u)}{u} + \frac{1}{6u}\frac{d\phi_{3\pi}^\sigma(u)}{du}\right) + \frac{1}{m_b^2 - q^2}\psi_{4\pi}(u)\right\}. \quad (4.9)$$

Here the contributions of twist-2 and of three-particle DA's vanish altogether. Combining (4.4) and (4.8) one is able to calculate the scalar $B \to \pi$ form factor:

$$f_{B\pi}^0(q^2) = f_{B\pi}^+(q^2) + \frac{q^2}{m_B^2 - m_\pi^2} f^-(q^2)\,. \quad (4.10)$$

Finally, the LCSR for the penguin form factor obtained from the third dispersion relation in (4.1) has the following expression:

$$f^T_{B\pi}(q^2) = \frac{(m_B+m_\pi)e^{m_B^2/M^2}}{2m_B^2 f_B}\left[F^T_0(q^2,M^2,s_0^B) + \frac{\alpha_s C_F}{4\pi}F^T_1(q^2,M^2,s_0^B)\right], \qquad (4.11)$$

where

$$F^T_0(q^2,M^2,s_0^B) = m_b f_\pi \int\limits_{u_0}^{1} du\, e^{-\frac{m_b^2-q^2\bar{u}}{uM^2}} \left\{ \frac{\varphi_\pi(u)}{u} - \frac{m_b\mu_\pi}{3(m_b^2-q^2)}\frac{d\phi^\sigma_{3\pi}(u)}{du} \right.$$
$$\left. + \frac{1}{m_b^2-q^2}\left(\frac{1}{4}\frac{d\phi_{4\pi}(u)}{du} - \frac{m_b^2\, u}{2(m_b^2-q^2)}\frac{d^2\phi_{4\pi}(u)}{du^2} - I^T_{4\pi}(u)\right)\right\}, \qquad (4.12)$$

and

$$I^T_{4\pi}(u) = \frac{d}{du}\left(\int\limits_0^u d\alpha_1 \int\limits_{(u-\alpha_1)/(1-\alpha_1)}^{1} \frac{dv}{v}\left[2\Psi_{4\pi}(\alpha_i) - (1-2v)\Phi_{4\pi}(\alpha_i)\right.\right.$$
$$\left.\left. +2(1-2v)\widetilde{\Psi}_{4\pi}(\alpha_i) - \widetilde{\Phi}_{4\pi}(\alpha_i)\right]\Bigg|_{\substack{\alpha_2 = 1-\alpha_1-\alpha_3,\\ \alpha_3=(u-\alpha_1)/v}}\right). \qquad (4.13)$$

The NLO parts $\widetilde{F}_1$ and $m_b F^T_1$ in LCSR (4.8) and (4.11), respectively, are represented in the form similar to (4.7), and the corresponding imaginary parts are collected in App. B.

For f_B entering LCSR we use the well known two-point sum rule [24] obtained from the correlator of two $m_b\bar{q}i\gamma_5 b$ currents. The latest analyses of this sum rule can be found in [18, 25]; here we employ the $\overline{MS}$ version [18]. For consistency with LCSR, the sum rule for f_B is taken with $O(\alpha_s)$ accuracy. For convenience, this expression is written down in App. C.

Note that the expressions for LCSR in LO are slightly modified as compared to the ones presented in the previous papers. We prefer not to use the so-called "surface terms", which originate from the powers of $1/(m_b^2-(q+up))^n$ with $n>1$ in the correlation functions. Instead, we use a completely equivalent but more compact form, with derivatives of DA's.

The twist-2 NLO part of LCSR for $f^+_{B\pi}$, hence, the expressions for T_1 and $\mathrm{Im}T_1$ in App. B, after transition to the pole scheme (the additional expressions necessary for this transition are also presented in App. B) coincide with the ones obtained in [4]. We have also checked an exact numerical coincidence with the twist-2 NLO part of the sum rule in [5], written in a different analytical form. The explicit expressions for the amplitudes $T_1^{p,\sigma}$, $\widetilde{T}_1$, $\widetilde{T}_1^{p,\sigma}$, and T_1^T,$T_1^{Tp,\sigma}$ and their imaginary parts presented in App. B are new. The $O(\alpha_s)$ spectral density entering the LCSR for $f^+_{B\pi}$ is given in [10] in a different form, that is, with the u-integration performed, making an analytical comparison of our result with this expression very complicated. The numerical comparison is discussed below, in sect. 6. Furthermore, in [26] the LCSR for the form factor $f^0_{B\pi}$ was obtained, and the imaginary

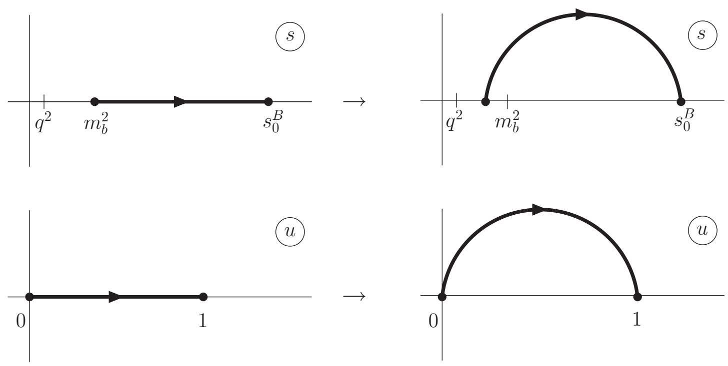

Figure 3: *Replacing the integration intervals by the contours in the complex planes of u and s variables in the alternative procedure of the numerical integration of NLO amplitudes.*

part of $\widetilde{T}_1$ was presented. A comparison with our expression for Im$\widetilde{T}_1$ reveals, however, some differences.

Since the imaginary parts of the hard-scattering amplitudes have a very cumbersome analytical structure, we carried out a special check of these expressions. Each hard-scattering amplitude $T_1, ...$ taken as a function of $u, q^2, (p+q)^2$ was numerically compared with its dispersion relation in the variable $(p+q)^2 = s$, where the expression for $\text{Im}_s T_1, ...$ was substituted. Note that one has to perform one subtraction in order to render the dispersion integral convergent.

In addition, we applied a new method which completely avoids the use of explicit imaginary parts of hard-scattering amplitudes, allowing one to numerically calculate the NLO parts of LCSR, e.g., $F_1(q^2, M^2, s_0^B)$ in (4.7), analytically continuing integrals to the complex plane. We make use of the fact that the hard-scattering amplitudes T_1, T_1^p, T_1^σ are analytical functions of the variable $s = (p+q)^2$ in the upper half of the complex plane, because of $i\epsilon$'s in Feynman propagators. Consider, as an example the twist-2 part of F_1 given by the integral over s in the second line of (4.7). Since the integration is performed along the real axis, the operation of taking the imaginary part can be moved outside the integral. To proceed, one has to shift the lower limit of the s-integration to any point at $q^2 < s < m_b^2$. This is legitimate because all T_1's are real at $s < m_b^2$. Then one deforms the path of the s-integration, replacing it by a contour in the upper half of the complex plane, as shown schematically in Fig. 3, so that all poles and cuts are away from the integration region. Only when s is approaching the upper limit s_0^B, one nears the pole at $u = (m_b^2 - q^2)/(s_0^B - q^2)$ while performing the integration over u. Because this pole does not touch the limits $u = 0, 1$, it is possible to avoid it by moving the contour of the u-integration into the upper half of the complex u-plane (see Fig. 3). After that, both numerical integrations become completely stable. Note, that in both s- and u-integrations, we integrate over the semi-circle, but the contour of the integration can be deformed in an arbitrary way in the upper half of the complex plane. The numerical integrations of T_1 over these contours yield an imaginary part which represents the desired answer for F_1. We have checked that the numerical results obtained by this alternative method coincide with

twist	Parameter	Value at $\mu = 1$ GeV	Source
2	a_2^π	0.25 ± 0.15	average from [19]
	a_4^π	$-a_2^\pi + (0.1 \pm 0.1)$	$\pi\gamma\gamma^*$ form factor [30]
	$a_{>4}^\pi$	0	
3	μ_π	$1.74^{+0.67}_{-0.38}$ GeV	GMOR relation; $m_{u,d}$ from [28]
	$f_{3\pi}$	0.0045 ± 0.0015 GeV^2	2-point QCD SR [19]
	$\omega_{3\pi}$	-1.5 ± 0.7	2-point QCD SR[19]
4	δ_π^2	0.18 ± 0.06 GeV^2	2-point QCD SR [19]
	ϵ_π	$\frac{21}{8}(0.2 \pm 0.1)$	2-point QCD SR [19]

Table 1: *Input parameters for the pion DA's.*

the ones obtained by the direct integration over the imaginary parts, thereby providing an independent check.

5. Numerical results

Let us specify the input parameters entering the LCSR (4.4), (4.8) and (4.11) for $B \to \pi$ form factors and the two-point sum rule (C.1) for f_B.

The value of the b-quark mass is taken from one of the most recent determinations [27]:

$$\overline{m}_b(\overline{m}_b) = 4.164 \pm 0.025 \text{ GeV}\,, \tag{5.1}$$

based on the bottomonium sum rules in the four-loop approximation. Note that (5.1) has a smaller uncertainty than the average over the non-lattice determinations given in [28]: $\overline{m}_b(\overline{m}_b) = 4.20 \pm 0.07$ GeV. However, as we shall see below, the uncertainty of $\overline{m}_b(\overline{m}_b)$ does not significantly influence the "error budget" of the final prediction. Furthermore, in our calculation, the scale-dependence $\overline{m}_b(\mu_m)$ is taken into account in the one-loop approximation which is sufficient for the $O(\alpha_s)$-accuracy of the correlation function. Note that using the $\overline{MS}$ mass inevitably introduces some scale-dependence of the lower threshold m_b^2 in the dispersion integrals in both LCSR and f_B sum rule. However, this does not create a problem, because the imaginary part of the OPE correlation function obtained from a fixed-order perturbative QCD calculation is not an observable, but only serves as an approximation for the hadronic spectral density.

The QCD coupling $\alpha_s(\mu_r)$ is obtained from $\alpha_s(m_Z) = 0.1176 \pm 0.002$ [28], with the NLO evolution to the renormalization scale μ_r. In addition to μ_m and μ_r, one encounters the factorization scale μ_f in the correlation function, at which the pion DA's are taken. In what follows, we adopt a single scale $\mu = \mu_m = \mu_r = \mu_f$ in both LCSR and two-point SR for f_B. The numerical value of μ will be specified below.

The input parameters of the twist-2 pion DA include $f_\pi = 130.7$ MeV [28] and the two first Gegenbauer moments a_2^π and a_4^π normalized at a low scale 1 GeV. For the latter we adopt the intervals presented in Table 1. The range for $a_2^\pi(1\text{GeV})$ is an average [19] over various recent determinations, including, e.g., $a_2^\pi(1\text{GeV}) = 0.26^{+0.21}_{-0.09}$ calculated from the two-point sum rule in [29]. For a_4^π we use, following [10], the constraint $a_2^\pi(1\text{GeV}) + a_4^\pi(1\text{GeV}) = 0.1 \pm 0.1$, obtained [30] from the analysis of $\pi\gamma\gamma^*$ form factor. Having in mind, that at large scales the renormalization suppresses all higher Gegenbauer moments, we set $a^\pi_{>4} = 0$ in our ansatz for $\varphi_\pi(u)$ specified in App. A. The uncertainties of $a^\pi_{2,4}(1\text{GeV})$ remain large, hence we neglect very small effects of their NLO evolution taken into account in [4].

The normalization parameter $\mu_\pi(1\text{GeV})$ of the twist-3 two-particle DA's presented in Table 1 is obtained adopting the (non-lattice) intervals [28] for the light quark masses: $m_u(2\text{ GeV}) = 3.0 \pm 1.0$ MeV, $m_d(2\text{ GeV}) = 6.0 \pm 1.5$ MeV. Correspondingly, the quark-condensate density given by GMOR relation is:

$$\langle \bar{q}q\rangle(1\text{GeV}) = -\frac{1}{2} f_\pi^2 \mu_\pi(1\text{GeV}) = -(246^{+28}_{-19}\text{ MeV})^3\,, \tag{5.2}$$

where very small $O(m^2_{u,d})$ corrections are neglected. We prefer to use the above range, rather than a narrower "standard" interval $\langle \bar{q}q\rangle(1\text{GeV}) = -(240 \pm 10\text{ MeV})^3$ employed in the previous analyses. In fact, (5.2) is consistent with $\langle \bar{q}q\rangle(1\text{GeV}) = (254 \pm 8\text{ MeV})^3$ quoted in the review [31], as well as with the recent determination of the light-quark masses from QCD sum rules with $O(\alpha_s^4)$ accuracy [32]: $m_u(2\text{ GeV}) = 2.7 \pm 0.4$ MeV, $m_d(2\text{ GeV}) = 4.8 \pm 0.5$ MeV.

The remaining parameters of the twist-3 DA's ($f_{3\pi}$, $\omega_{3\pi}$) and twist-4 DA's (δ^2_π, ϵ_π) presented in Table 1 are taken from [19], where they are calculated from auxiliary two-point sum rules. The latter are obtained from the vacuum correlation functions containing the local quark-gluon operators that enter the matrix elements (A.6), (A.7) and (A.12), (A.13). The one-loop running for all parameters of DA's is taken into account using the scale-dependence relations presented in App. A. Note that the small value of $f_{3\pi}$ effectively suppresses all nonasymptotic and three-particle contributions of the twist-3 DA's. Furthermore, the overall size of the twist-4 contributions to LCSR is very small. Hence, although the parameters of the twist-3,4 DA's have large uncertainties, only the accuracy of μ_π plays a role in LCSR[1]. Finally, in the sum rule (C.1) for f_B the gluon condensate density $\langle \alpha_s/\pi GG\rangle = 0.012^{+0.006}_{-0.012}$ GeV^4 and the ratio of the quark-gluon and quark-condensate densities $m_0^2 = 0.8 \pm 0.2$ GeV^2 [31] are used, the accuracy of these parameters playing a minor role.

The universal parameters listed above determine the "external" input for sum rules. The next step is to specify appropriate intervals for the "internal" parameters: the scale μ, the Borel parameters M and $\overline{M}$ and the effective thresholds s_0^B and $\overline{s}_0^B$. In doing that, we take all external input parameters at their central values, allowing only a_2^π and a_4^π to vary within the intervals given in Table 1.

From previous studies [4, 5, 8, 10] it is known that an optimal renormalization scale is $\mu \sim \sqrt{m_B^2 - m_b^2} \sim \sqrt{2m_b\bar{\Lambda}}$ (where $\bar{\Lambda}$ does not scale with the heavy quark mass),

[1] We also expect that the use of the recently developed renormalon model [33] for the twist-4 DA's, instead of the "conventional" twist-4 DA's [34] used here, will not noticeably change the numerical results.

and simultaneously, μ has the order of magnitude of the Borel scales defining the average virtuality in the correlation functions. In practice, M and $\overline{M}$ are varied within the "working windows" of the respective sum rules, hence one expects that also μ has to be taken in a certain interval.

Calculating the total Borel-transformed correlation function (that is, the $s_0^B \to \infty$ limit of LCSR) we demand that the contribution of subleading twist-4 terms remains very small, $< 3\%$ of the LO twist-2 term, thereby diminishing the contributions of the higher twists, that are not taken into account in the OPE. This condition puts a lower bound $M^2 \geq M^2_{min} = 15$ GeV^2. In addition, in order to keep the α_s-expansion in the Borel-transformed correlation function under control, both NLO twist-2 and twist-3 terms are kept $\leq 30\%$ of their LO counterparts, yielding a lower limit $\mu \geq 2.5$ GeV. Hereafter a "default" value $\mu = 3$ GeV is used.

Furthermore, we determine the effective threshold parameter s_0^B in LCSR for each $M^2 \geq M^2_{min}$. We refrain from using equal threshold parameters in LCSR and two-point sum rule for f_B, as it was done earlier, e.g. in [4, 8]. Instead, we control the duality approximation by calculating certain observables directly from LCSR and fitting them to their measured values. Importantly, we include in the fitting procedure not only s_0^B, but also the two least restricted external parameters a_2^π and a_4^π, under the condition that both Gegenbauer moments remain within the intervals of their direct determination given in Table 1.

The first observable used in this analysis is the B-meson mass. In a similar way, as e.g., in [10, 18], m_B^2 is calculated taking the derivative of LCSR over $-1/M^2$ and dividing it by the original sum rule. The B-meson mass extracted from LCSR has to deviate from its experimental value $m_B = 5.279$ GeV by less than 1 %. Secondly, we make use of the recent rather accurate measurement of the q^2-distribution in $B \to \pi l \nu$ by BABAR collaboration [35]. We remind that LCSR for $B \to \pi$ form factors are valid up to momentum transfers $q^2 \sim m_b^2 - 2m_b\bar{\Lambda}$, typically at $0 < q^2 < 14 - 15$ GeV^2. To be on the safe side, we take the maximal allowed q^2 slightly lower than in the previous analyses and calculate the slope $f^+_{B\pi}(q^2)/f^+_{B\pi}(0)$ from LCSR at $0 < q^2 < 12$ GeV^2. The obtained ratio is then fitted to the slope of the form factor inferred from the data. We employ the result of [36], where various parameterizations of the form factor $f^+_{B\pi}(q^2)$ are fitted to the measured q^2-distribution. Since all fits turn out to be almost equally good, we adopt the simplest BK-parameterization [37]:

$$\frac{f^{+(BK)}_{B\pi}(q^2)}{f^{+(BK)}_{B\pi}(0)} = \frac{1}{(1 - q^2/m^2_{B^*})(1 - \alpha_{BK} q^2/m_B^2)} \tag{5.3}$$

with the slope parameter $\alpha_{BK} = 0.53 \pm 0.06$ from [36] (close to α_{BK} fitted in [35]).

After fixing s_0^B for each accessible M^2, we demand that heavier hadronic states contribute less than 30% of the ground-state B meson contribution to LCSR. This condition yields an upper limit $M^2 < M^2_{max} = 21$ GeV^2. The resulting spread of the threshold parameter and Gegenbauer moments when M^2 varies between M^2_{min} and M^2_{max} is very small: $s_0^B = 36 - 35.5$ GeV^2, $a_2^\pi(1\text{GeV}) = 0.15 - 0.17$, $a_4^\pi(1\text{GeV}) = 0.05 - 0.03$. The

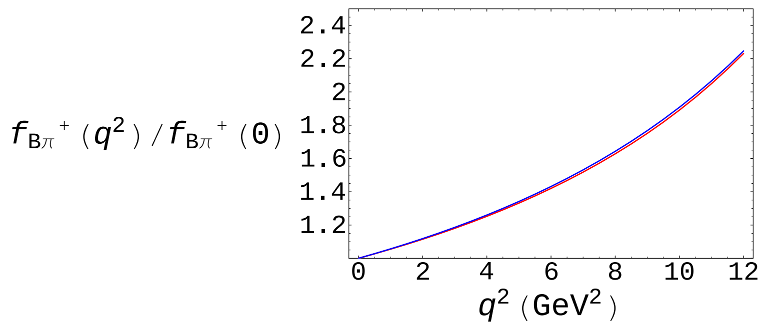

Figure 4: *The LCSR prediction for the form factor shape $f^+_{B\pi}(q^2)/f^+_{B\pi}(0)$ fitted to the BK parameterization of the measured q^2-distribution. The two (almost indistinguishable) curves are the fit and the parameterization (5.3) at $\alpha_{BK} = 0.53$.*

quality of the fit is illustrated in Fig. 4 where the two curves: the calculated q^2-shape of the form factor and the BK-parameterization (5.3) are almost indistinguishable. Thus, in our numerical analysis we "trade" the q^2-dependence predicted from LCSR for a smaller uncertainty of the Gegenbauer moments and for a better control over the quark-hadron duality approximation.

In the final stage of the numerical analysis we turn to the two-point QCD sum rule for f_B presented in App. C and find that at the adopted value of the renormalization scale $\mu = 3$ GeV the interval $\overline{M}^2 = 5.0 \pm 1.0$ GeV^2 satisfies the same criteria as the ones imposed in the numerical analysis of LCSR: the smallness of higher power terms in OPE, and suppression of the heavier hadronic contributions. The threshold parameter $\overline{s}_0^B = 35.6^{-0.9}_{+2.1}$ GeV^2 is fixed by calculating m_B^2 from this sum rule. This time the deviation from the experimental value is even less than 0.5 %. For completeness, we quote the resulting interval $f_B = 214^{-5}_{+7}$ MeV. Note that the $O(\alpha_s^2)$ correction taken into account in [18] is not included here. As usual, employing the sum rule for f_B in order to extract the form factor from the LCSR for the product $f_B f^+_{B\pi}$ turns out to be extremely useful. One observes a partial cancellation of the α_s-corrections in both LCSR and two-point sum rule and a better stability with respect to the variation of scales.

To demonstrate some important numerical features of the LCSR prediction, in Fig. 5 (left) we plot the M^2-dependence of the form factor $f^+_{B\pi}(0)$ with all other inputs fixed at their central values. The observed stability, far beyond the adopted "working" interval in M^2, serves as a usual criterion of reliability in QCD sum rule approach. The μ-dependence plotted in Fig. 5 (right) is very mild from $\mu = 2.5$ GeV up to $\mu = 6$ GeV. The numerical size of the gluon radiative corrections in LCSR is illustrated in Fig. 6.

The numerical analysis yields the following prediction for the vector $B \to \pi$ form factor

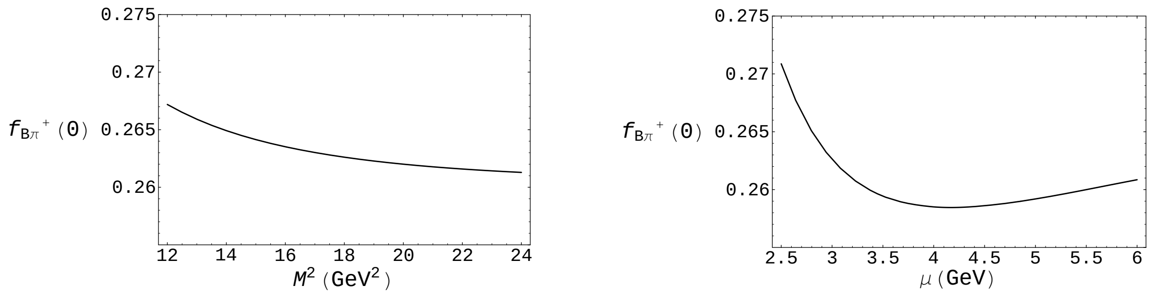

Figure 5: *Dependence of $f^+_{B\pi}(0)$ on the Borel parameter (left) and renormalization scale (right).*

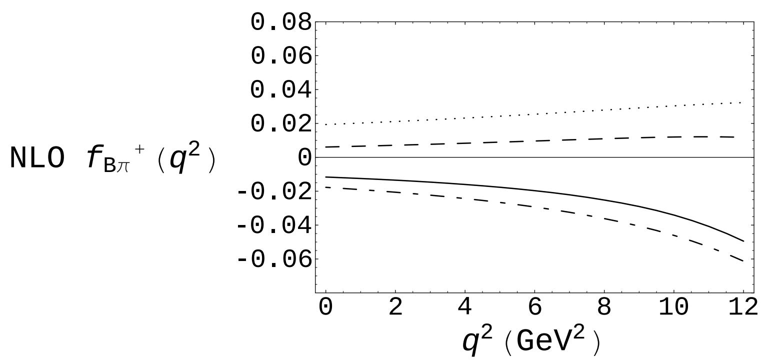

Figure 6: *Gluon radiative corrections to the twist-2 (dotted line) and twist-3 (solid line) parts of LCSR for $f^+_{B\pi}(q^2)$, as a function of q^2. The part proportional to ϕ_σ (ϕ_p) is shown separately by dashed (dash-dotted) line.*

at zero momentum transfer:

$$f^+_{B\pi}(0) = 0.263 \left.{}^{+0.004}_{-0.005}\right|_{M,\overline{M}} \left.{}^{+0.009}_{-0.004}\right|_{\mu} \pm 0.02\Big|_{shape} \left.{}^{+0.03}_{-0.02}\right|_{\mu_\pi} \pm 0.001\Big|_{m_b}\,, \tag{5.4}$$

where the central value is calculated at $\mu = 3.0$ GeV, $M^2 = 18.0$ GeV^2, $s_0^B = 35.75$ GeV^2, $a_2^\pi(1\text{GeV}) = 0.16$, $a_4^\pi(1\text{GeV}) = 0.04$, $\overline{M}^2 = 5.0$ GeV^2 and $\overline{s}_0^B = 35.6$ GeV^2. The percentages of different contributions to the central value in (5.4) are presented in Table 2.

In (5.4) the first (second) uncertainties are due to the variation of the Borel parameters M and $\overline{M}$ (scale μ) within the intervals specified above. The third uncertainty reflects the error of the experimental slope parameter. In addition, we quote the uncertainties due to limited knowledge of the "external" input parameters. We have estimated them by simply varying these parameters one by one within their intervals and fixing the central values for all "internal" input parameters. Interestingly, the largest uncertainty of order of 10% is due to the error in the determination of light-quark masses transformed into the uncertainty of μ_π, the coefficient of the large twist-3 LO contribution. The spread caused by the current uncertainty of $\overline{m}_b(\overline{m}_b)$ is much smaller, hence, does not influence the resulting total uncertainty, even if one increases the error of m_b-determination by a factor of two. Remaining theoretical errors caused by the current uncertainties of α_s, twist-3,4 DA's parameters and higher-dimensional condensates are very small, and for brevity they are not shown in (5.4).

b-quark mass	$\overline{MS}$	pole
input	central	set II from [10]
$f^+_{B\pi}(0)$	0.263	0.258
tw2 LO	50.5%	39.7%
tw2 NLO	7.4%	17.2 %
tw3 LO	46.7%	41.5 %
tw3 NLO	-4.4%	2.4 %
tw4 LO	-0.2%	-0.9%

Table 2: *The form factor $f^+_{B\pi}$ at zero momentum transfer calculated from LCSR in two different quark-mass schemes and separate contributions to the sum rule in %.*

Finally, we add all uncertainties in quadrature and obtain the interval:

$$f^+_{B\pi}(0) = 0.26^{+0.04}_{-0.03}\,, \tag{5.5}$$

which is our main numerical result. It can be used to normalize the experimentally measured shape, e.g., the one in (5.3), yielding the form factor $f^+_{B\pi}(q^2)$ in the whole q^2-range of $B \to \pi l \nu_l$.

With this prediction at hand, we are in a position to extract $|V_{ub}|$. For that we use the interval

$$|V_{ub}| f^+_{B\pi}(0) = \left(9.1 \pm 0.6\big|_{shape} \pm 0.3\big|_{BR}\right) \times 10^{-4}\,, \tag{5.6}$$

inferred [36] from the measured q^2-shape [35] and average branching fraction of $B \to \pi l \nu_l$ [38]. We obtain:

$$|V_{ub}| = \left(3.5 \pm 0.4\big|_{th} \pm 0.2\big|_{shape} \pm 0.1\big|_{BR}\right) \times 10^{-3}\,, \tag{5.7}$$

where the first error is due to the estimated uncertainty of $f^+_{B\pi}(0)$ in (5.5), and the two remaining errors originate from the experimental errors in (5.6). A possible small correlation between the shape uncertainty of our prediction for the form factor and the experimental shape uncertainty is not taken into account.

The remaining two $B \to \pi$ form factors can now be predicted without any additional input. In particular, we adopt the same Borel parameter M^2 and effective threshold s_0^B, assuming that they only depend on the quantum numbers of the interpolating current for B meson. The scalar form factor $f^0_{B\pi}(q^2)$, obtained by combining the LCSR for $f^+_{B\pi}$ and $(f^+_{B\pi}+f^-_{B\pi})$, and the penguin form factor $f^T_{B\pi}(q^2)$ are presented in Fig. 7, in comparison with $f^+_{B\pi}(q^2)$. The predicted interval for the penguin form factor at zero momentum transfer is :

$$f^T_{B\pi}(0) = 0.255 \pm 0.035\,, \tag{5.8}$$

adopting $\mu = 3$ GeV as the renormalization scale of the penguin current.

6. Discussion

In this paper, we returned to the LCSR for the $B \to \pi$ form factors. We recalculated the $O(\alpha_s)$ gluon radiative corrections to the twist-2 and twist-3 hard-scattering amplitudes and

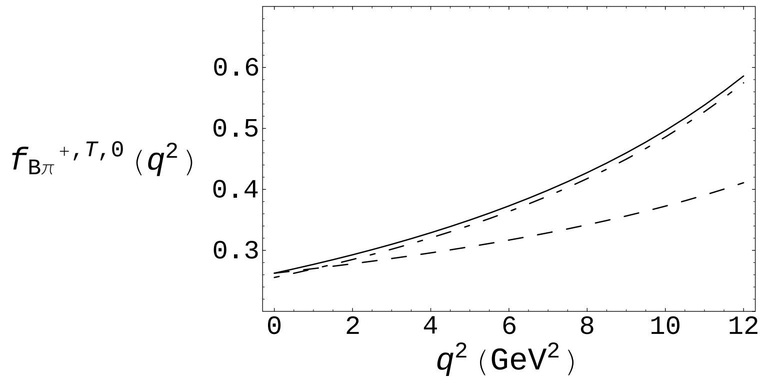

Figure 7: *The LCSR prediction for form factors $f^+_{B\pi}(q^2)$ (solid line), $f^0_{B\pi}(q^2)$ (dashed line) and $f^T_{B\pi}(q^2)$ (dash-dotted line) at $0 < q^2 < 12$ GeV^2 and for the central values of all input parameters.*

presented the first complete set of expressions for these amplitudes and their imaginary parts. For the radiative corrections to the twist-2 part of the LCSR for $f^+_{B\pi}$ we reproduced the results of [4, 5]. For the radiative corrections to the twist-3 part we confirmed the cancellation of infrared divergences observed in [9, 10] in the case of asymptotic DA's. Including the nonasymptotic effects in these radiative corrections demands taking into account the mixing between two- and three-particle DA's. In fact, the parameter $f_{3\pi}$ determining the size of nonasymptotic twist-3 corrections is numerically small, hence these corrections are not expected to influence the numerical results.

Throughout our calculation and in the final sum rule relations we used the $\overline{MS}$-mass of the b quark, which is the most suitable mass definition for short-distance hard-scattering amplitudes. Indeed, as follows from our numerical analysis, the $O(\alpha_s)$ corrections to the sum rules turn out to be comparably small. To demonstrate that, we returned to the pole-mass scheme in LCSR and used exactly the same input as in [10] (the preferred "set 2" with $m_b^{pole} = 4.8\,\text{GeV}$). We calculated the total form factor and separate contributions to the sum rule in both quark-mass schemes and compared them in Table 2. Note that the twist-2 NLO correction is distinctively smaller in the $\overline{MS}$-mass scheme. In the twist-3 part of the sum rule the α_s-correction is small in both schemes. In the $\overline{MS}$ scheme, as seen from Fig. 6, this correction is dominated by the contribution of the DA $\phi^p_{3\pi}$. In the pole scheme there is a partial cancellation between the contributions of the two twist-3 DA's. Our numerical results for the form factors $f^{+,0,T}_{B\pi}(q^2)$ in the pole scheme are very close to the ones obtained in [10]. It is however difficult to compare separate contributions, because they are not presented in [10]. We also cannot confirm the numerical values of the twist-3 NLO corrections to the form factor $f^+_{B\pi}(q^2)$ plotted in the figure presented in the earlier publication [9].

Further improvements of LCSR are possible but demand substantial calculational efforts. For example, obtaining radiative corrections to the three-particle twist-3,4 contributions is technically very difficult. Again, we expect no visible change of the predicted form factors because three-particle terms are already very small in LO. A more feasible task is to go beyond twist-4 in OPE and estimate the twist-5,6 effects, related to the four-particle pion DA's, at least in the factorization approximation, where one light quark-antiquark pair is replaced by the quark condensate (In LCSR for the pion electromagnetic form factor these estimates have been done in [39]).

The numerical analysis of LCSR was improved due to the use of the q^2-shape measurement in $B \to \pi l \nu$. A smaller theoretical uncertainty of LCSR predictions can be anticipated with additional data on this shape, as well as with more accurate determinations of b- and, especially, u, d-quark masses.

In this paper, all calculations have been done in full QCD with a finite b-quark mass. At the same time, the whole approach naturally relies on the fact that m_b is a very large scale as compared with Λ_{QCD} and related nonperturbative parameters. Our results demonstrate that the twist-hierarchy as well as the perturbative expansion of the correlation function work reasonably well. An interesting problem is the investigation of the $m_b \to \infty$ limit of LCSR and various aspects of this limiting transition, e.g., the hierarchy of radiative and nonasymptotic corrections. This problem remaining out of our scope was already discussed in several papers: earlier, in [7] at the LO level, in [5],[40] at NLO level and more recently, in [16].

[ref.]	$f^+_{B\pi}(q^2)$ calculation	$f^+_{B\pi}(q^2)$ input	$\|V_{ub}\| \times 10^3$
[41]	lattice ($n_f = 3$)	-	3.78±0.25±0.52
[42]	lattice ($n_f = 3$)	-	3.55±0.25±0.50
[43]	-	lattice ⊕ SCET $B \to \pi\pi$	$3.54 \pm 0.17 \pm 0.44$
[44]	-	lattice	$3.7 \pm 0.2 \pm 0.1$
[45]	-	lattice ⊕ LCSR	$3.47 \pm 0.29 \pm 0.03$
[10, 36]	LCSR	-	$3.5 \pm 0.4 \pm 0.1$
this work	LCSR	-	$3.5 \pm 0.4 \pm 0.2 \pm 0.1$

Table 3: *Recent $|V_{ub}|$ determinations from $B \to \pi l \nu_l$*

Finally, in Table 3 we compare our result for $|V_{ub}|$ with the one of the previous LCSR analysis and with the recent lattice QCD determinations obtained at large q^2 and extrapolated to small q^2 with the help of various parameterizations. The observed mutual agreement ensures confidence in the continuously improving V_{ub} determination from exclusive B decays.

Acknowledgments

We are grateful to Th. Feldmann, M. Jamin and R. Zwicky for useful discussions. This work was supported by the Deutsche Forschungsgemeinschaft (Project KH 205/1-2). The work of G.D and B.M was supported by the Ministry of Science, Education and Sport of the Republic of Croatia, under contract 098-0982930-2864. The partial support of A. von Humboldt Foundation under the Program of Institute Partnership is acknowledged. The work of N.O. was supported by FLAVIAnet (Contract No. MRTN-CT-2006-035482).

A. Pion distribution amplitudes

For convenience, we specify the set of the pion DA's and their parameters used in this paper. The notations and parameters for twist-3 and 4 DA's are taken from [19], where the earlier studies [34, 46] are updated.

The two-particle DA's of the pion enter the following decomposition of the bilocal vacuum-pion matrix element (for definiteness, π^+ in the final state):

$$\langle\pi^+(p)|\bar u^i_\omega(x_1)d^j_\xi(x_2)|0\rangle_{x^2\to 0} = \frac{i\delta^{ij}}{12}f_\pi\int_0^1 du\; e^{iup\cdot x_1+i\bar u p\cdot x_2}\Bigg([\not p\gamma_5]_{\xi\omega}\varphi_\pi(u)$$
$$-[\gamma_5]_{\xi\omega}\mu_\pi\phi^p_{3\pi}(u)+\frac{1}{6}[\sigma_{\beta\tau}\gamma_5]_{\xi\omega}p_\beta(x_1-x_2)_\tau\mu_\pi\phi^\sigma_{3\pi}(u)$$
$$+\frac{1}{16}[\not p\gamma_5]_{\xi\omega}(x_1-x_2)^2\phi_{4\pi}(u)-\frac{i}{2}[(\not x_1-\not x_2)\gamma_5]_{\xi\omega}\int\limits_0^u\psi_{4\pi}(v)dv\Bigg)\,, \qquad \text{(A.1)}$$

In the above, the product of the quark fields is expanded near the light-cone, that is, $x_i=\xi_i x$, where ξ_i are arbitrary numbers, and $x^2=0$; $\bar u = 1-u$. The path-ordered gauge-factor (Wilson line) is omitted assuming the fixed-point gauge for the gluons. The light-cone expansion includes the twist-2 DA φ_π, two twist-3 DA's $\phi^p_{3\pi}$, $\phi^\sigma_{3\pi}$ and two twist-4 DA's $\phi_{4\pi}$ and $\psi_{4\pi}$. The usual definitions of DA's are easily obtained, multiplying both parts of (A.1) by the corresponding combinations of γ matrices and taking Dirac and color traces.

The decomposition of the three-particle quark-antiquark-gluon matrix element is:

$$\langle\pi^+(p)|\bar u^i_\omega(x_1)g_sG^a_{\mu\nu}(x_3)d^j_\xi(x_2)|0\rangle_{x^2\to 0}=\frac{\lambda^a_{ji}}{32}\int\mathcal{D}\alpha_i e^{ip(\alpha_1x_1+\alpha_2x_2+\alpha_3x_3)}$$
$$\times\Bigg[if_{3\pi}(\sigma_{\lambda\rho}\gamma_5)_{\xi\omega}(p_\mu p_\lambda g_{\nu\rho}-p_\nu p_\lambda g_{\mu\rho})\Phi_{3\pi}(\alpha_i)$$
$$-f_\pi(\gamma_\lambda\gamma_5)_{\xi\omega}\Big\{(p_\nu g_{\mu\lambda}-p_\mu g_{\nu\lambda})\Psi_{4\pi}(\alpha_i)+\frac{p_\lambda(p_\mu x_\nu-p_\nu x_\mu)}{(p\cdot x)}\left(\Phi_{4\pi}(\alpha_i)+\Psi_{4\pi}(\alpha_i)\right)\Big\}$$
$$-\frac{if_\pi}{2}\epsilon_{\mu\nu\delta\rho}(\gamma_\lambda)_{\xi\omega}\Big\{(p^\rho g^{\delta\lambda}-p^\delta g^{\rho\lambda})\widetilde\Psi_{4\pi}(\alpha_i)+\frac{p_\lambda(p^\delta x^\rho-p^\rho x^\delta)}{(p\cdot x)}\left(\widetilde\Phi_{4\pi}(\alpha_i)+\widetilde\Psi_{4\pi}(\alpha_i)\right)\Big\}\Bigg]\,. \qquad \text{(A.2)}$$

including one twist-3 DA $\Phi_{3\pi}$ and four twist-4 DA's : $\Phi_{4\pi}$, $\Psi_{4\pi}$, $\widetilde\Phi_{4\pi}$ and $\widetilde\Psi_{4\pi}$. Here the convention $\epsilon^{0123}=-1$ is used, which corresponds to $Tr\{\gamma^5\gamma^\mu\gamma^\nu\gamma^\alpha\gamma^\beta\}=4i\epsilon^{\mu\nu\alpha\beta}$.

The following expressions for the DA's entering the decompositions (A.1) and (A.2) are used:

- twist-2 DA:
$$\varphi_\pi(u)=6u\bar u\Big(1+a_2C^{3/2}_2(u-\bar u)+a_4C^{3/2}_4(u-\bar u)\Big)\,, \qquad \text{(A.3)}$$
where, according to our choice, the first two Gegenbauer polynomials are included in the nonasymptotic part, with the coefficients having the following LO scale depen-

dence:

$$a_2(\mu_2) = [L(\mu_2,\mu_1)]^{\frac{25C_F}{6\beta_0}}\, a_2(\mu_1), \quad a_4(\mu_2) = [L(\mu_2,\mu_1)]^{\frac{91C_F}{15\beta_0}}\, a_4(\mu_1) \tag{A.4}$$

with $L(\mu_2,\mu_1) = \alpha_s(\mu_2)/\alpha_s(\mu_1)$, $\beta_0 = 11 - 2n_f/3$.

- twist-3 DA's :

$$\Phi_{3\pi}(\alpha_i) = 360\alpha_1\alpha_2\alpha_3^2 \left[1 + \frac{\omega_{3\pi}}{2}(7\alpha_3 - 3)\right] \tag{A.5}$$

with the nonperturbative parameters $f_{3\pi}$ and $\omega_{3\pi}$ defined via matrix elements of the following local operators:

$$\langle\pi^+(p)|\bar{u}\sigma_{\mu\nu}\gamma_5 G_{\alpha\beta} d|0\rangle = i f_{3\pi}\Big[(p_\alpha p_\mu g_{\beta\nu} - p_\beta p_\mu g_{\alpha\nu}) - (p_\alpha p_\nu g_{\beta\mu} - p_\beta p_\nu g_{\alpha\mu})\Big], \tag{A.6}$$

$$\langle\pi^+(p)|\bar{u}\sigma_{\mu\lambda}\gamma_5[D_\beta, G_{\alpha\lambda}]d - \frac{3}{7}\partial_\beta \bar{u}\sigma_{\mu\lambda}\gamma_5 G_{\alpha\lambda} d|0\rangle = -\frac{3}{14} f_{3\pi}\omega_{3\pi} p_\alpha p_\beta p_\mu \,. \tag{A.7}$$

The scale dependence of the twist-3 parameters is given by:

$$\mu_\pi(\mu_2) = [L(\mu_2,\mu_1)]^{-\frac{4}{\beta_0}}\, \mu_\pi(\mu_1)\,, \quad f_{3\pi}(\mu_2) = [L(\mu_2,\mu_1)]^{\frac{1}{\beta_0}\left(\frac{7C_F}{3}+3\right)}\, f_{3\pi}(\mu_1)\,, \tag{A.8}$$

$$(f_{3\pi}\omega_{3\pi})(\mu_2) = [L(\mu_2,\mu_1)]^{\frac{1}{\beta_0}\left(\frac{7C_F}{6}+10\right)}\, (f_{3\pi}\omega_{3\pi})(\mu_1)\,. \tag{A.9}$$

The corresponding expressions for the twist-3 quark-antiquark DA are:

$$\begin{aligned} \phi^p_{3\pi}(u) &= 1 + 30\frac{f_{3\pi}}{\mu_\pi f_\pi} C_2^{1/2}(u-\bar{u}) - 3\frac{f_{3\pi}\omega_{3\pi}}{\mu_\pi f_\pi} C_4^{1/2}(u-\bar{u}), \\ \phi^\sigma_{3\pi}(u) &= 6u(1-u)\left(1 + 5\frac{f_{3\pi}}{\mu_\pi f_\pi}\left(1 - \frac{\omega_{3\pi}}{10}\right) C_2^{3/2}(u-\bar{u})\right). \end{aligned} \tag{A.10}$$

- twist-4 DA's:

$$\begin{aligned} \Phi_{4\pi}(\alpha_i) &= 120\delta_\pi^2\varepsilon_\pi(\alpha_1-\alpha_2)\alpha_1\alpha_2\alpha_3 \ , \\ \Psi_{4\pi}(\alpha_i) &= 30\delta_\pi^2(\mu)(\alpha_1-\alpha_2)\alpha_3^2[\frac{1}{3} + 2\varepsilon_\pi(1-2\alpha_3)] \ , \\ \widetilde{\Phi}_{4\pi}(\alpha_i) &= -120\delta_\pi^2\alpha_1\alpha_2\alpha_3[\frac{1}{3} + \varepsilon_\pi(1-3\alpha_3)] \ , \\ \widetilde{\Psi}_{4\pi}(\alpha_i) &= 30\delta_\pi^2\alpha_3^2(1-\alpha_3)[\frac{1}{3} + 2\varepsilon_\pi(1-2\alpha_3)] \ , \end{aligned} \tag{A.11}$$

are the four three-particle DA's, where the nonperturbative parameters δ_π^2 and ϵ_π are defined as

$$\langle\pi^+(p)|\bar{u}\widetilde{G}_{\alpha\mu}\gamma^\alpha d|0\rangle = i\delta_\pi^2 f_\pi p_\mu \,, \tag{A.12}$$

and (up to twist 5 corrections):

$$\langle\pi^+(p)|\bar{u}[D_\mu, \widetilde{G}_{\nu\xi}]\gamma^\xi d - \frac{4}{9}\partial_\mu \bar{u}\widetilde{G}_{\nu\xi}\gamma^\xi d|0\rangle = -\frac{8}{21} f_\pi\delta_\pi^2\epsilon_\pi p_\mu p_\nu \,, \tag{A.13}$$

with the scale-dependence:

$$\delta_\pi^2(\mu_2) = [L(\mu_2,\mu_1)]^{\frac{8C_F}{3\beta_0}}\, \delta_\pi^2(\mu_1)\,, \quad (\delta_\pi^2\epsilon_\pi)(\mu_2) = [L(\mu_2,\mu_1)]^{\frac{10}{\beta_0}}\, (\delta_\pi^2\epsilon_\pi)(\mu_1)\,. \tag{A.14}$$

Note that the twist-4 parameter $\omega_{4\pi}$ introduced in [19] is replaced by $\epsilon_\pi = (21/8)\omega_{4\pi}$. Correspondingly, the two-particle DA's of twist 4 are:

$$\phi_{4\pi}(u) = \frac{200}{3}\delta_\pi^2 u^2\bar{u}^2 + 8\delta_\pi^2\epsilon_\pi\Big\{u\bar{u}(2+13u\bar{u}) + 2u^3(10-15u+6u^2)\ln u + 2\bar{u}^3(10-15\bar{u}+6\bar{u}^2)\ln\bar{u}\Big\}, \tag{A.15}$$

$$\psi_{4\pi}(u) = \frac{20}{3}\delta_\pi^2 C_2^{1/2}(2u-1). \tag{A.16}$$

These DA's are related to the original definitions [34] as

$$\phi_{4\pi}(u) = 16\Big(g_1(u) - \int\limits_0^u g_2(v)dv\Big), \quad \psi_{4\pi}(u) = -2\frac{dg_2(u)}{du}. \tag{A.17}$$

B. Formulae for gluon radiative corrections

Here we collect the expressions for the hard-scattering amplitudes entering the factorization formulae (3.1) and the resulting imaginary parts of these amplitudes determining the radiative correction (4.7) to LCSR (4.4) for $f^+_{B\pi}$, as well as the analogous expressions for LCSR (4.8) and (4.11) for the other two form factors.

To compactify the formulae, we use the dimensionless variables

$$r_1 = \frac{q^2}{m_b^2}, \quad r_2 = \frac{(p+q)^2}{m_b^2}, \tag{B.1}$$

(in the imaginary parts $r_2 = s/m_b^2$) and the integration variable :

$$\rho = r_1 + u(r_2 - r_1) \qquad \int\limits_0^1 du = \int\limits_{r_1}^{r_2} \frac{d\rho}{r_2 - r_1}, \tag{B.2}$$

and introduce the combinations of logarithmic functions

$$G(x) = \mathrm{Li}_2(x) + \ln^2(1-x) + \ln(1-x)\left(\ln\frac{m_b^2}{\mu^2} - 1\right), \tag{B.3}$$

where $\mathrm{Li}_2(x) = -\int_0^x \frac{dt}{t}\ln(1-t)$ is the Spence function, and

$$L_1(x) = \ln\left(\frac{(x-1)^2}{x}\frac{m_b^2}{\mu^2}\right) - 1, \quad L_2(x) = \ln\left(\frac{(x-1)^2}{x}\frac{m_b^2}{\mu^2}\right) - \frac{1}{x}. \tag{B.4}$$

The imaginary parts of the hard-scattering amplitudes are taken at fixed $q^2 < m_b^2$ ($r_1 < 1$), analytically continuing these amplitudes in the variable $s = (p+q)^2$ (or r_2). The result contains combinations of $\theta(1-\rho)$, $\theta(\rho-1)$ and $\delta(\rho-1)$ and its derivatives. To isolate the spurious infrared divergences which one encounters by taking the imaginary part, we follow [4] and introduce the usual plus-prescription

$$\int_{r_1}^{r_2} d\rho \left(\left\{\begin{matrix}\theta(1-\rho)\\ \theta(\rho-1)\end{matrix}\right\}\frac{g(\rho)}{\rho-1}\right)_+ \phi(\rho) = \int_{r_1}^{r_2} d\rho \left\{\begin{matrix}\theta(1-\rho)\\ \theta(\rho-1)\end{matrix}\right\}\frac{g(\rho)}{\rho-1}\Big(\phi(\rho)-\phi(1)\Big), \tag{B.5}$$

for generic functions $\phi(\rho)$, $g(\rho)$. Furthermore, to make the formulae for imaginary parts more explicit, we partially integrate the derivatives of $\delta(\rho-1)$ using, e.g.:

$$\int_{r_1}^{r_2} d\rho\, \delta'(\rho-1)\phi(\rho) = \int d\rho \delta(\rho-1) \left(-\frac{d}{d\rho} + \delta(r_2-1)\right) \phi(\rho)\,, \tag{B.6}$$

omitting the terms with $\delta(r_2-1)$ in all cases where $\phi(1)=0$.

B.1 Amplitudes for $f^+_{B\pi}$ LCSR

$$\begin{aligned}
\frac{1}{2}T_1 =& \left(\frac{1}{\rho-1} - \frac{r_2-1}{(r_2-r_1)^2 u}\right) G(r_1) + \left(\frac{1}{\rho-1} + \frac{1-r_1}{(r_2-r_1)^2(1-u)}\right) G(r_2) \\
&- \left(\frac{2}{\rho-1} - \frac{r_2-1}{(r_2-r_1)^2 u} + \frac{1-r_1}{(r_2-r_1)^2(1-u)}\right) G(\rho) \\
&+ \frac{1}{r_2}\left(\frac{r_2-1}{\rho-1} - \frac{r_2-1}{(r_2-r_1)(1-u)}\right) \ln(1-r_2) \\
&+ \frac{1}{r_2}\left(\frac{r_2-2}{2\rho} - \frac{r_2}{2\rho^2} + \frac{r_2-1}{(r_2-r_1)(1-u)}\right) \ln(1-\rho) \\
&+ \frac{\rho+1}{2(\rho-1)^2}\left(3\ln\left(\frac{m_b^2}{\mu^2}\right) - \frac{3\rho+1}{\rho}\right),
\end{aligned} \tag{B.7}$$

$$\begin{aligned}
-\frac{1}{2\pi}\mathrm{Im}_s T_1 =& \,\theta(1-\rho)\left[\frac{1-r_1}{(r_2-r_1)(r_2-\rho)} L_1(r_2) + \left(\frac{L_2(r_2)}{\rho-1}\right)_+ + \frac{1}{(r_2-\rho)}\left(\frac{1}{r_2}-1\right)\right] \\
&+ \theta(\rho-1)\left[\frac{1-r_1}{(r_2-r_1)(r_2-\rho)} L_1(r_2) + \frac{1+\rho-r_1-r_2}{(r_1-\rho)(r_2-\rho)} L_1(\rho) + \left(\frac{L_2(r_2)-2L_1(\rho)}{\rho-1}\right)_+ \right.\\
&\left. + \frac{1}{2\rho}\left(1-\frac{1}{\rho}-\frac{2}{r_2}\right)\right] \\
&+ \delta(\rho-1)\left[\left(\ln\frac{r_2-1}{1-r_1}\right)^2 - \left(\frac{1}{r_2} - 1 + \ln r_2\right)\ln\frac{(r_2-1)^2}{1-r_1} + \frac{1}{2}\left(4-3\ln\left(\frac{m_b^2}{\mu^2}\right)\right)\right. \\
&\left. + \mathrm{Li}_2(r_1) - 3\,\mathrm{Li}_2(1-r_2) + 1 - \frac{\pi^2}{2} - \left(4-3\ln\left(\frac{m_b^2}{\mu^2}\right)\right)\left(1+\frac{d}{d\rho}\right)\right],
\end{aligned} \tag{B.8}$$

$$
\begin{aligned}
\frac{r_2-r_1}{2}T_1^p = &\left(\frac{1}{\rho-1}-\frac{4r_1-1}{(r_2-r_1)u}\right)G(r_1)-\left(\frac{r_1}{\rho-1}+\frac{1+r_1+r_2}{(r_2-r_1)(1-u)}\right)G(r_2)\\
&+\left(-\frac{1-r_1}{\rho-1}+\frac{1+r_1+r_2}{(r_2-r_1)(1-u)}+\frac{4r_1-1}{(r_2-r_1)u}\right)G(\rho)\\
&-\left(\frac{r_1}{\rho-1}+\frac{2r_1}{(r_2-r_1)u}\right)\ln(1-r_1)\\
&+\frac{1}{r_2}\left(\frac{r_1+r_2-r_1r_2}{\rho-1}+\frac{r_1-r_2-r_2(r_1+r_2)}{(r_2-r_1)(1-u)}\right)\ln(1-r_2)\\
&+\frac{1}{2}\left(\frac{3(3-r_1)}{\rho-1}+\frac{6(1-r_1)}{(\rho-1)^2}-1\right)\ln\left(\frac{m_b^2}{\mu^2}\right)\\
&+\left(\frac{1-r_1}{\rho-1}-\frac{1}{2}-\frac{r_1-r_2-r_2(r_1+r_2)}{r_2(r_2-r_1)(1-u)}+\frac{2r_1}{(r_2-r_1)u}\right.\\
&\left.-\frac{2r_1+r_2-3r_1r_2}{2r_2\rho}-\frac{r_1}{2\rho^2}\right)\ln(1-\rho)+\frac{2(r_1-3)}{\rho-1}+\frac{1}{2}-\frac{r_1}{2\rho}-\frac{4(1-r_1)}{(\rho-1)^2}\,,
\end{aligned}
\tag{B.9}
$$

$$
\begin{aligned}
\frac{r_2-r_1}{2\pi}\mathrm{Im}_sT_1^p = &\,\theta(1-\rho)\left[\frac{1+r_2}{r_2(r_2-\rho)}+\frac{1+r_1+r_2}{r_2-\rho}L_2(r_2)-(1-r_1L_2(r_2))\left(\frac{1}{\rho-1}\right)_+\right]\\
&+\theta(\rho-1)\left[\frac{1+r_1+r_2}{r_2-\rho}L_1(r_2)-\left(\frac{4r_1-1}{\rho-r_1}-\frac{1+r_1+r_2}{\rho-r_2}\right)L_1(\rho)\right.\\
&\quad\left.+\left(\frac{r_1L_2(r_2)+(1-r_1)\,L_1(\rho)+r_1-2}{\rho-1}\right)_+ +\frac{1}{2}+\frac{2r_1+r_2-3r_1r_2}{2r_2\rho}+\frac{r_1}{2\rho^2}+\frac{2r_1}{r_1-\rho}\right]\\
&+\delta(\rho-1)\left[-\left(\ln\frac{r_2-1}{1-r_1}\right)^2+(r_1+1)\ln\left(\frac{r_2-1}{1-r_1}\right)L_1(r_2)\right.\\
&\quad-\ln(r_2-1)\left(2\frac{r_1}{r_2}+3(1-r_1)+(r_1-1)\ln r_2\right)+\ln(1-r_1)\left(\frac{r_1}{r_2}+1-\ln r_2\right)\\
&\quad-\frac{\pi^2}{6}(4r_1+1)+\frac{1}{2}(r_1-3)\left(3\ln\left(\frac{m_b^2}{\mu^2}\right)-4\right)-\mathrm{Li}_2(r_1)+(1-2r_1)\mathrm{Li}_2(1-r_2)\\
&\quad\left.+(1-r_1)\left(4-3\ln\left(\frac{m_b^2}{\mu^2}\right)\right)\left(\frac{d}{d\rho}-\delta(r_2-1)\right)\right]\,,
\end{aligned}
\tag{B.10}
$$

$$
\begin{aligned}
3T_1^\sigma =& \left(-\frac{1}{(\rho-1)^2}+\frac{2(1-2r_1)}{(1-r_1)(\rho-1)}-\frac{1-4r_1}{(r_2-r_1)^2u^2}-\frac{2(1-2r_1)}{(1-r_1)(r_2-r_1)u}\right)G(r_1)\\
&+\left(-\frac{r_1}{(\rho-1)^2}+\frac{2r_2}{(r_2-1)(\rho-1)}+\frac{1+r_1+r_2}{(r_2-r_1)^2(1-u)^2}+\frac{2r_2}{(r_2-r_1)(r_2-1)(1-u)}\right)G(r_2)\\
&+\left(\frac{1+r_1}{(\rho-1)^2}+\frac{2(1-2r_1-2r_2+3r_1r_2)}{(1-r_1)(r_2-1)(\rho-1)}-\frac{1+r_1+r_2}{(r_2-r_1)^2(1-u)^2}+\frac{1-4r_1}{(r_2-r_1)^2u^2}\right.\\
&-\left.\frac{2r_2}{(r_2-r_1)(r_2-1)(1-u)}+\frac{2(1-2r_1)}{(1-r_1)(r_2-r_1)u}\right)G(\rho)\\
&+\left(-\frac{r_1}{(\rho-1)^2}+\frac{2r_1}{(r_2-r_1)^2u^2}\right)\ln(1-r_1)+\left(\frac{r_1-r_2-r_1r_2}{r_2(\rho-1)^2}\right.\\
&+\left.\frac{4}{\rho-1}-\frac{r_1-r_2-r_2(r_1+r_2)}{r_2(r_2-r_1)^2(1-u)^2}+\frac{4}{(r_2-r_1)(1-u)}\right)\ln(1-r_2)\\
&-\left(\frac{3(1+r_1)}{(\rho-1)^2}+\frac{1+3r_2+8r_1-10r_1r_2-3r_1^2+r_1^2r_2}{(1-r_1)(r_2-1)(\rho-1)}+\frac{r_2^2+r_1r_2+r_2-r_1}{r_2(r_2-r_1)^2(1-u)^2}\right.\\
&+\frac{2r_1}{(r_2-r_1)^2u^2}+\frac{5r_2^2+r_1r_2-2r_2+r_1+1}{r_2(r_2-r_1)(r_2-1)(1-u)}-\frac{1-3r_1-4r_1^2}{r_1(1-r_1)(r_2-r_1)u}\\
&+\left.\frac{r_1}{\rho^3}+\frac{2r_1-r_2-3r_1r_2}{2r_2\rho^2}+\frac{r_2r_1^2-r_1^2-r_2r_1-r_1+r_2}{r_1r_2\rho}\right)\ln(1-\rho)\\
&-\left(\frac{6(1+r_1)}{(\rho-1)^3}+\frac{5r_1-3}{2(\rho-1)^2}+\frac{1+r_2+3r_1-4r_1r_2-r_1^2}{(1-r_1)(r_2-1)(\rho-1)}\right.\\
&+\left.\frac{1+r_1+r_2}{(r_2-r_1)(r_2-1)(1-u)}-\frac{1-4r_1}{(1-r_1)(r_2-r_1)u}\right)\ln\left(\frac{m_b^2}{\mu^2}\right)\\
&-\frac{1-4r_1-r_2+3r_1r_2+2r_1^2-r_1^2r_2}{(1-r_1)(r_2-1)(\rho-1)}+\frac{r_1}{r_2(r_2-r_1)(r_2-1)(1-u)}\\
&-\frac{1-2r_1}{(1-r_1)(r_2-r_1)u}+\frac{8(1+r_1)}{(\rho-1)^3}-\frac{2(1-2r_1)}{(\rho-1)^2}-\frac{r_1}{\rho^2}+\frac{2r_1(r_2-1)+r_2}{2r_2\rho}\,, \qquad \text{(B.11)}
\end{aligned}
$$

$$
\begin{aligned}
\frac{3}{\pi}\mathrm{Im}_s T_1^\sigma \; = \; & \theta(1-\rho)\Bigg[(1+r_1L_2(r_2))\left(\frac{1}{\rho-1}\right)_+\frac{d}{d\rho}-2\left(1+\frac{r_2L_2(r_2)}{r_2-1}\right)\left(\frac{1}{\rho-1}\right)_+ \\
& -\left(\frac{1+r_1+r_2}{(\rho-r_2)^2}-\frac{2r_2}{(r_2-1)(\rho-r_2)}\right)L_2(r_2)-\frac{1+r_2}{r_2(\rho-r_2)^2}+\frac{2}{\rho-r_2}\Bigg] \\
& +\theta(\rho-1)\Bigg[\left((1+r_1)\left(\frac{1-L_1(\rho)}{\rho-1}\right)_+ +(1+r_1L_2(r_2))\left(\frac{1}{\rho-1}\right)_+\right)\frac{d}{d\rho} \\
& +2\left(3+\frac{1}{r_2-1}-\frac{1}{1-r_1}\right)\left(\frac{L_1(\rho)}{\rho-1}\right)_+ \\
& +\left(-\frac{2r_2}{r_2-1}L_2(r_2)+\frac{1+r_1}{\rho}+\frac{2(2+r_1)}{r_2-1}+\frac{1-8r_1+r_1^2}{1-r_1}\right)\left(\frac{1}{\rho-1}\right)_+ \\
& -\left(\frac{1+r_1+r_2}{(\rho-r_2)^2}-\frac{2r_2}{(r_2-1)(\rho-r_2)}\right)L_2(r_2) \\
& -\left(\frac{1-4r_1}{(r_1-\rho)^2}+2\frac{1-2r_1}{(r_1-1)(r_1-\rho)}+\frac{2r_2}{(r_2-1)(\rho-r_2)}-\frac{1+r_1+r_2}{(r_2-\rho)^2}\right)L_1(\rho) \\
& +\frac{r_1}{\rho^3}+\frac{2r_1}{(r_1-\rho)^2}-\frac{3r_2^2+r_1r_2+r_1+1}{r_2(r_2-1)(\rho-r_2)}+\frac{(r_2-1)(1+r_1+r_2)}{r_2(r_2-\rho)^2} \\
& -\frac{r_2+r_1(3r_2-2)}{2r_2\rho^2}-\frac{r_1(-r_2r_1+r_1+r_2+1)-r_2}{r_1r_2\rho}+\frac{(1+r_1)(1-4r_1)}{r_1(1-r_1)(r_1-\rho)}\Bigg] \\
& +\delta(\rho-1)\Bigg[\frac{\pi^2}{3}\left(\frac{1}{2}(1-4r_1)\frac{d}{d\rho}+\frac{3-2r_1}{1-r_1}+\frac{4}{r_2-1}\right) \\
& +\Big[\ln^2(1-r_1)-(1-2r_1)\ln^2(r_2-1)+\mathrm{Li}_2(r_1)-(1+2r_1)\mathrm{Li}_2(1-r_2) \\
& -\left(2-r_1-\frac{r_1}{r_2}+2r_1\ln(r_2-1)-r_1\ln r_2\right)\ln(1-r_1) \\
& +2\left(2+r_1-\frac{r_1}{r_2}-r_1\ln r_2\right)\ln(r_2-1)+2(2-r_1) \\
& +\left(-\frac{5-3r_1}{2}+(1-r_1)\ln\frac{1-r_1}{r_2-1}\right)\ln\left(\frac{m_b^2}{\mu^2}\right)\Big]\frac{d}{d\rho} \\
& -2\left(2-\frac{1}{1-r_1}\right)\ln^2(1-r_1)-2\left(\frac{1}{1-r_1}+\frac{2}{r_2-1}\right)\ln^2(r_2-1) \\
& -2\left(2-\frac{1}{1-r_1}\right)\mathrm{Li}_2(r_1)+2\left(3-\frac{1}{1-r_1}+\frac{r_2+1}{r_2-1}\right)\mathrm{Li}_2(1-r_2) \\
& -2+r_1\left(1-\frac{1}{r_2-1}\right)+\frac{1}{1-r_1} \\
& -2\left(-3+\frac{1}{r_2-1}+\frac{1}{1-r_1}+\frac{r_2}{r_2-1}\ln r_2-\frac{2r_2}{r_2-1}\ln(r_2-1)\right)\ln(1-r_1) \\
& -2\left(\frac{2}{1-r_1}-\frac{3+r_1}{r_2-1}-\frac{2r_2}{r_2-1}\ln r_2\right)\ln(r_2-1) \\
& +\Bigg(4-\frac{3}{1-r_1}+\frac{2+r_1}{r_2-1}-2\left(2-\frac{r_2}{r_2-1}-\frac{1}{1-r_1}\right)\ln(1-r_1) \\
& -2\left(\frac{1}{r_2-1}+\frac{r_1}{1-r_1}\right)\ln(r_2-1)\Bigg)\ln\left(\frac{m_b^2}{\mu^2}\right) \\
& -(1+r_1)\left(4-3\ln\left(\frac{m_b^2}{\mu^2}\right)\right)\left(\frac{d^2}{d\rho^2}-\delta(r_2-1)\frac{d}{d\rho}\right)\Bigg]\,. \qquad \text{(B.12)}
\end{aligned}
$$

As already mentioned, the above formulae are obtained in the $\overline{MS}$ scheme. To switch to the one-loop pole mass of b quark the following expressions

$$\Delta T_1 = -\frac{2\rho\left(3\ln\left(\frac{m_b^2}{\mu^2}\right)-4\right)}{(\rho-1)^2}\,, \tag{B.13}$$

$$\Delta T_1^p = \frac{(r_1-\rho)(\rho+1)\left(3\ln\left(\frac{m_b^2}{\mu^2}\right)-4\right)}{(r_2-r_1)(\rho-1)^2}\,, \tag{B.14}$$

$$\Delta T_1^\sigma = \frac{((3-2\rho)\rho+r_1(\rho+3)+3)\left(3\ln\left(\frac{m_b^2}{\mu^2}\right)-4\right)}{6(\rho-1)^3}\,. \tag{B.15}$$

have to be added to the hard-scattering amplitudes T_1, T_1^p and T_1^σ. respectively. The corresponding additions to the imaginary parts are

$$\frac{1}{2\pi}\mathrm{Im}_s\Delta T_1 = \delta(\rho-1)\left(3\ln\left(\frac{m_b^2}{\mu^2}\right)-4\right)\left(1+\frac{d}{d\rho}\right)\,, \tag{B.16}$$

$$\frac{r_2-r_1}{2\pi}\mathrm{Im}_s\Delta T_1^p = \delta(\rho-1)\left(3\ln\left(\frac{m_b^2}{\mu^2}\right)-4\right)\left(\frac{3-r_1}{2}+(1-r_1)\left(\frac{d}{d\rho}-\delta(r_2-1)\right)\right)\,, \tag{B.17}$$

$$\begin{aligned}\frac{3}{\pi}\mathrm{Im}\Delta_s T_1^\sigma = \delta(\rho-1)\left(3\ln\left(\frac{m_b^2}{\mu^2}\right)-4\right)\Bigg(1&+\frac{1-r_1}{2}\frac{d}{d\rho}\\ &-(1+r_1)\left(\frac{d^2}{d\rho^2}-\delta(r_2-1)\frac{d}{d\rho}\right)\Bigg)\,.\end{aligned} \tag{B.18}$$

B.2 Amplitudes for $(f^+_{B\pi}+f^-_{B\pi})$ LCSR

$$\begin{aligned}\widetilde{T}_1 = {}& \frac{r_1^2-r_1r_2-(1-r_1)(r_2-r_1)\ln(1-r_1)}{r_1^2(\rho-1)}+\frac{(1-r_1)(r_1+r_2)\ln(1-r_1)}{r_1^2(r_2-r_1)u}\\ &-\frac{2(r_2-1)\ln(1-r_2)}{r_2(1-u)(r_2-r_1)}+\frac{(\rho-1)(r_2+\rho)\ln(1-\rho)}{(r_2-r_1)(1-u)u\rho^2}+\frac{r_2-r_1}{r_1\rho}\,,\end{aligned} \tag{B.19}$$

$$\begin{aligned}\frac{1}{\pi}\mathrm{Im}_s\widetilde{T}_1 = {}& \theta(1-\rho)\left[\frac{2(r_2-1)}{r_2(r_2-\rho)}\right]\\ &+\theta(\rho-1)\frac{1}{r_1-\rho}\left[\frac{r_1-r_2}{\rho^2}-\frac{(2-r_2)(r_2-r_1)}{r_2\rho}+\frac{2(r_2-1)}{r_2}\right]\\ &+\delta(\rho-1)\left[\frac{r_2}{r_1}+\frac{(r_1-1)(r_1-r_2)\ln(1-r_1)}{r_1^2}-1\right]\,,\end{aligned} \tag{B.20}$$

$$\begin{aligned}\widetilde{T}_1^p = {}& \frac{4G(r_1)}{(r_2-r_1)u}+\frac{2(r_2-1)G(r_2)}{(r_2-r_1)(1-u)(\rho-1)}-\left(\frac{4}{(r_2-r_1)u}+\frac{2}{\rho-1}+\frac{2}{(r_2-r_1)(1-u)}\right)G(\rho)\\ &+\left(\frac{2(r_1+1)}{r_1(r_2-r_1)u}-\frac{1-2r_1-r_1^2}{r_1^2(\rho-1)}\right)\ln(1-r_1)+\left(\frac{2(r_2-1)}{r_2(\rho-1)}+\frac{2(r_2-1)}{(r_2-r_1)r_2(1-u)}\right)\ln(1-r_2)\\ &+\frac{2(\rho+2)}{(\rho-1)^2}\ln\left(\frac{m_b^2}{\mu^2}\right)+\left(-\frac{2(r_1+1)}{r_1(r_2-r_1)u}-\frac{2(r_2-1)}{(r_2-r_1)r_2(1-u)}+\frac{2}{\rho-1}+\frac{r_2r_1+2r_1+2r_2}{r_1r_2\rho}\right.\\ &\left.-\frac{4}{\rho}+\frac{1}{\rho^2}\right)\ln(1-\rho)+\frac{1}{\rho}-\frac{1+3r_1}{r_1(\rho-1)}-\frac{8}{(\rho-1)^2}\,,\end{aligned} \tag{B.21}$$

$$
\begin{aligned}
\frac{1}{\pi}\mathrm{Im}_s\widetilde{T}_1^p =\ & \theta(1-\rho)\left[2\frac{r_2-1}{\rho-r_2}L_2(r_2)\left(\frac{1}{\rho-1}\right)_+\right] + \theta(\rho-1)\left[-2\left(1+\frac{1-r_2}{\rho-r_2}L_2(r_2)\right)\left(\frac{1}{\rho-1}\right)_+\right.\\
& +2\left(\frac{L_1(\rho)}{\rho-1}\right)_+ + \frac{2(-r_1+2r_2-\rho)}{(r_1-\rho)(\rho-r_2)}L_1(\rho) - \frac{2r_1+2r_2-3r_2r_1}{r_1r_2\rho} + 2\frac{(r_1+1)}{r_1(\rho-r_1)}\\
& \left.-2\frac{r_2-1}{r_2(\rho-r_2)} - \frac{1}{\rho^2}\right]\\
& +\delta(\rho-1)\left[2\left(\ln(r_2)+\frac{2}{r_2}-3\right)\ln(r_2-1) + \left(\frac{1}{r_1^2}-\frac{r_1(2-r_1)}{r_1^2}-\frac{2}{r_2}\right)\ln(1-r_1)\right.\\
& -2\ln\left(\frac{r_2-1}{1-r_1}\right)L_1(r_2) + 4\mathrm{Li}_2(1-r_2) + \frac{1}{r_1} + 3 - 2\ln\left(\frac{m_b^2}{\mu^2}\right) + \frac{4}{3}\pi^2\\
& \left.+2\left(4-3\ln\left(\frac{m_b^2}{\mu^2}\right)\right)\left(\frac{d}{d\rho}-\delta(r_2-1)\right)\right],
\end{aligned}
\tag{B.22}
$$

$$
\begin{aligned}
\widetilde{T}_1^\sigma =\ & \frac{2(r_1-1)G(r_1)}{3u^2(\rho-1)(r_1-r_2)} + \left(\frac{r_2-r_1}{3(\rho-1)^2} - \frac{1}{3(r_2-r_1)(1-u)^2}\right)G(r_2)\\
& +\left(\frac{2(r_2-r_1)}{3(r_1-1)(\rho-1)} + \frac{2}{3(1-r_1)u} - \frac{r_2-r_1}{3(\rho-1)^2} + \frac{1}{3(1-u)^2(r_2-r_1)}\right.\\
& \qquad \left.+\frac{2}{3u^2(r_2-r_1)}\right)G(\rho)\\
& +\left(\frac{1+r_1}{3r_1(r_1-r_2)u^2} + \frac{1}{3r_1^2u} + \frac{r_2-r_1}{3r_1^2(1-\rho)} - \frac{r_1^3-r_2r_1^2+r_1-r_2}{6r_1^2(\rho-1)^2}\right)\ln(1-r_1)\\
& +\left(\frac{r_2^2-r_1r_2-r_2+r_1}{3r_2(\rho-1)^2} - \frac{r_2-1}{3r_2(r_2-r_1)(1-u)^2}\right)\ln(1-r_2)\\
& +\left(\frac{1-r_1}{3r_1(r_2-r_1)u^2} + \frac{1+r_2}{3(r_2-1)r_2(1-u)} + \frac{(r_2-r_1)\left((r_2-1)r_1^2-2r_2r_1+r_2\right)}{3r_1^2r_2\rho}\right.\\
& +\frac{1}{3(r_2-r_1)(1-u)^2} - \frac{1}{3r_2(r_2-r_1)(1-u)^2} + \frac{2}{3(r_2-r_1)u^2} + \frac{r_2-r_1}{(\rho-1)^2}\\
& +\frac{(r_2-r_1)(2-3r_2)}{6r_2\rho^2} + \frac{r_2-r_1}{3\rho^3} + \frac{3r_1-1}{3r_1^2u(1-r_1)} + \frac{2}{3u(1-r_1)} + \frac{2(r_2-r_1)}{3(\rho-1)(r_1-1)}\\
& \left.+\frac{(r_1(r_2-3)-3r_2+5)(r_2-r_1)}{3(r_2-1)(\rho-1)(1-r_1)}\right)\ln(1-\rho)\\
& +\left(\frac{2(r_2-r_1)}{(\rho-1)^3} + \frac{1}{3(r_2-1)(1-u)} + \frac{2}{3(1-r_1)u}\right.\\
& \qquad \left.+\frac{-r_1^2-r_2r_1+3r_1+2r_2^2-3r_2}{3(r_1-1)(r_2-1)(\rho-1)} + \frac{2(r_2-r_1)}{3(\rho-1)^2}\right)\ln\left(\frac{m_b^2}{\mu^2}\right)\\
& +\frac{1}{3r_2(1-r_2)(1-u)} + \frac{1}{3r_1u} + \frac{-r_2r_1^2+2r_1^2+r_2^2r_1-r_2r_1-r_1-r_2^2+r_2}{3r_1(r_2-1)(\rho-1)}\\
& +\frac{-r_2^2+r_1r_2+r_2-r_1}{3r_2\rho} - \frac{-7r_1^2+7r_2r_1+r_1-r_2}{6r_1(\rho-1)^2} + \frac{r_2-r_1}{3\rho^2} + \frac{8(r_2-r_1)}{3(1-\rho)^3},
\end{aligned}
\tag{B.23}
$$

$$
\begin{aligned}
\frac{3}{r_2-r_1}\frac{1}{\pi}\mathrm{Im}_s\widetilde{T}_1^\sigma =\; & \theta(1-\rho)\left[\frac{L_2(r_2)}{(r_2-\rho)^2}-L_2(r_2)\left(\frac{1}{\rho-1}\right)_+\frac{d}{d\rho}\right] \\
& +\theta(\rho-1)\left[\left(\frac{L_1(\rho)-L_2(r_2)-1}{\rho-1}\right)_+\frac{d}{d\rho}+\frac{L_2(r_2)}{(r_2-\rho)^2}\right. \\
& +\left(-\frac{2}{(r_1-\rho)^2}-\frac{1}{(r_2-\rho)^2}+\frac{2}{(r_1-1)(\rho-r_1)}\right)L_1(\rho) \\
& -2\left(\frac{3-r_1-2r_2}{(1-r_1)(r_2-1)}\right)\left(\frac{1}{\rho-1}\right)_+ +\frac{2}{1-r_1}\left(\frac{L_1(\rho)}{\rho-1}\right)_+ \\
& +\frac{1+r_2}{r_2(r_2-1)(\rho-r_2)}+\frac{r_1^2+2r_1r_2-r_2}{r_1^2r_2\rho} \\
& \left.+\frac{r_1(2r_1+3)-1}{(r_1-1)r_1^2(\rho-r_1)}+\frac{3r_2-2}{2r_2\rho^2}-\frac{1+r_1}{r_1(\rho-r_1)^2}+\frac{1-r_2}{r_2(\rho-r_2)^2}-\frac{1}{\rho^3}\right] \\
& +\delta(\rho-1)\left[\frac{\pi^2}{3}\left(2\frac{d}{d\rho}-\frac{1}{1-r_1}\right)-\Bigg(2\ln(r_2-1)\,(1-\ln(r_2-1)\right. \\
& +L_2(r_2))+\ln\left(\frac{m_b^2}{\mu^2}\right)(1-\ln(r_2-1))-2\mathrm{Li}_2(1-r_2) \\
& +\frac{1}{2}\ln(1-r_1)\left(1+\frac{1}{r_1^2}-2L_2(r_2)\right)+\frac{1}{2}\left(\frac{1}{r_1}-3\right)\Bigg)\frac{d}{d\rho} \\
& +\frac{2\ln(1-r_1)}{1-r_1}\left(1+\frac{1-r_1}{2r_1^2}-\ln(1-r_1)\right) \\
& +\frac{2\ln(r_2-1)}{1-r_1}\left(\ln(r_2-1)+\frac{r_1+r_2-2}{r_2-1}\right)+\frac{1}{r_2-1}+\frac{1}{r_1}-1 \\
& +\frac{2}{r_1-1}\left(-\frac{r_1+2r_2-3}{2(r_2-1)}+\ln(1-r_1)-\ln(r_2-1)\right)\ln\left(\frac{m_b^2}{\mu^2}\right) \\
& +\frac{2}{r_1-1}\left(\mathrm{Li}_2(r_1)-\mathrm{Li}_2(1-r_2)\right) \\
& \left.+\left(4-3\ln\left(\frac{m_b^2}{\mu^2}\right)\right)\left(\frac{d^2}{d\rho^2}-\delta(r_2-1)\frac{d}{d\rho}\right)\right]\,, \qquad \text{(B.24)}
\end{aligned}
$$

$$
\Delta\widetilde{T}_1 = 0\,, \qquad \text{(B.25)}
$$

$$
\Delta\widetilde{T}_1^p = -\frac{(\rho+1)\left(3\ln\left(\frac{m_b^2}{\mu^2}\right)-4\right)}{(\rho-1)^2}\,, \qquad \text{(B.26)}
$$

$$
\Delta\widetilde{T}_1^\sigma = -\frac{(r_2-r_1)(\rho+3)\left(3\ln\left(\frac{m_b^2}{\mu^2}\right)-4\right)}{6(\rho-1)^3}\,, \qquad \text{(B.27)}
$$

$$
\frac{1}{\pi}\mathrm{Im}_s\Delta\widetilde{T}_1^p = \delta(\rho-1)\left(3\ln\left(\frac{m_b^2}{\mu^2}\right)-4\right)\left(1+2\left(\frac{d}{d\rho}-\delta(r_2-1)\right)\right)\,, \qquad \text{(B.28)}
$$

$$
\frac{3}{r_2-r_1}\frac{1}{\pi}\mathrm{Im}_s\widetilde{T}_1^\sigma = \delta(\rho-1)\left(3\ln\left(\frac{m_b^2}{\mu^2}\right)-4\right)\left(\frac{1}{2}\frac{d}{d\rho}+\frac{d^2}{d\rho^2}-\delta(r_2-1)\frac{d}{d\rho}\right). \qquad \text{(B.29)}
$$

B.3 Amplitudes for $f^T_{B\pi}$ LCSR

$$\frac{1}{2}T_1^T = \left(\frac{1-r_1}{(r_2-r_1)(\rho-1)} - \frac{r_2-1}{(r_2-r_1)^2u} + \frac{r_2-1}{(r_2-r_1)(\rho-1)}\right)G(r_1)$$
$$+\left(\frac{1-r_1}{(r_2-r_1)^2(1-u)} + \frac{1}{\rho-1}\right)G(r_2) + \left(-\frac{1-r_1}{(r_2-r_1)^2(1-u)} + \frac{r_2-1}{(r_2-r_1)^2u} - \frac{2}{\rho-1}\right)G(\rho)$$
$$+\left(-\frac{1-r_1}{r_1(r_2-r_1)u} + \frac{1-r_1}{r_1(\rho-1)}\right)\ln(1-r_1)$$
$$+\left(\frac{r_2-1}{(r_2-r_1)r_2(1-u)} + \frac{r_2-1}{r_2(\rho-1)}\right)\ln(1-r_2)$$
$$+\left(-\frac{r_2-1}{(r_2-r_1)r_2(1-u)} + \frac{1}{2\rho^2} + \frac{1-r_1}{r_1(r_2-r_1)u} - \frac{-2r_1+r_2r_1+2r_2}{2r_1r_2\rho}\right)\ln(1-\rho)$$
$$+\left(-\frac{1}{2(\rho-1)} + \frac{3}{(\rho-1)^2}\right)\ln\left(\frac{m_b^2}{\mu^2}\right) + \frac{1}{\rho-1} + \frac{1}{2\rho} - \frac{4}{(\rho-1)^2}\,, \tag{B.30}$$

$$\frac{1}{2\pi}\mathrm{Im}_s T_1^T = \theta(1-\rho)\left[\frac{1-r_1}{(r_2-r_1)(\rho-r_2)}L_1(r_2) - L_2(r_2)\left(\frac{1}{\rho-1}\right)_+ + \frac{r_2-1}{r_2(\rho-r_2)}\right]$$
$$+\theta(\rho-1)\left[\frac{1-r_1}{(r_2-r_1)(\rho-r_2)}L_1(r_2) + \frac{r_1+r_2-\rho-1}{(r_1-\rho)(r_2-\rho)}L_1(\rho)\right.$$
$$\left.-L_2(r_2)\left(\frac{1}{\rho-1}\right)_+ + 2\left(\frac{L_1(\rho)}{\rho-1}\right)_+ + \frac{r_1-1}{r_1(\rho-r_1)} + \frac{2(r_2-r_1)+r_1r_2}{2r_1r_2\rho} - \frac{1}{2\rho^2}\right]$$
$$+\delta(\rho-1)\left[-\left(\ln\frac{r_2-1}{1-r_1}\right)^2 + \left(-\ln(r_2) - \frac{1}{r_1} - \frac{1}{r_2} + 2\right)\ln(1-r_1)\right.$$
$$+2\ln(r_2-1)\left(\ln(r_2) + \frac{1}{r_2} - 1\right) + \frac{1}{2}\ln\left(\frac{m_b^2}{\mu^2}\right) - \mathrm{Li}_2(r_1) + 3\,\mathrm{Li}_2(1-r_2)$$
$$\left.-1 + \frac{\pi^2}{2} + \left(4 - 3\ln\left(\frac{m_b^2}{\mu^2}\right)\right)\frac{d}{d\rho}\right]\,, \tag{B.31}$$

$$\frac{1}{2}T_1^{T\,p} = \left(-\frac{3}{(r_2-r_1)^2u} + \frac{1}{(r_2-r_1)(\rho-1)}\right)G(r_1)$$
$$-\left(\frac{1}{(r_2-r_1)(\rho-1)} + \frac{3}{(r_2-r_1)^2(1-u)}\right)G(r_2) + \frac{3G(\rho)}{(r_1-r_2)^2u(1-u)}$$
$$+\left(\frac{1-2r_1}{r_1(r_2-r_1)(\rho-1)} - \frac{2}{(r_2-r_1)^2u}\right)\ln(1-r_1)$$
$$+\left(\frac{1}{(r_2-r_1)r_2(\rho-1)} - \frac{2}{(r_2-r_1)^2(1-u)}\right)\ln(1-r_2)$$
$$+\left(\frac{2}{(r_2-r_1)\rho} + \frac{2}{(r_2-r_1)^2u(1-u)}\right)\ln(1-\rho)\,, \tag{B.32}$$

$$
\begin{aligned}
\frac{r_2-r_1}{2\pi}\mathrm{Im}_s T_1^{T\,p} = {} & \theta(1-\rho)\left[\frac{3}{r_2-\rho}L_1(r_2)+(L_2(r_2)-1)\left(\frac{1}{\rho-1}\right)_+ + \frac{2}{r_2-\rho}\right] \\
& + \theta(\rho-1)\left[\frac{3}{r_2-\rho}L_1(r_2)+\frac{3(r_1-r_2)}{(r_2-\rho)(\rho-r_1)}L_1(\rho)\right. \\
& \left. +(L_2(r_2)-1)\left(\frac{1}{\rho-1}\right)_+ - \frac{2(r_1-2\rho)}{(r_1-\rho)\rho}\right] \\
& - \delta(\rho-1)\left[\ln^2(1-r_1)+\left(2\ln(r_2-1)-\ln(r_2)+\frac{1}{r_1}-\frac{1}{r_2}-4\right)\ln(1-r_1)\right. \\
& -3\ln^2(r_2-1)+2\ln(r_2-1)\left(\ln(r_2)+\frac{1}{r_2}+1\right) \\
& \left. -2\left(\ln\frac{r_2-1}{1-r_1}\right)\ln\left(\frac{m_b^2}{\mu^2}\right)+\mathrm{Li}_2(r_1)+\mathrm{Li}_2(1-r_2)+\frac{5\pi^2}{6}\right], \qquad \text{(B.33)}
\end{aligned}
$$

$$
\begin{aligned}
\frac{1}{2}T_1^{T\,\sigma} = {} & \left(\frac{-1}{3(1-r_1)(\rho-1)}-\frac{1}{6(\rho-1)^2}+\frac{1}{3(1-r_1)(r_2-r_1)u}+\frac{1}{2(r_2-r_1)^2u^2}\right)G(r_1) \\
& +\left(\frac{1}{3(r_2-1)(\rho-1)}-\frac{1}{6(\rho-1)^2}+\frac{1}{3(r_2-r_1)(r_2-1)(1-u)}\right. \\
& \left. +\frac{1}{2(r_2-r_1)^2(1-u)^2}\right)G(r_2) \\
& +\left(\frac{r_1+r_2-2}{3(1-r_1)(r_2-1)(\rho-1)}-\frac{1}{3(r_2-r_1)(r_2-1)(1-u)}-\frac{1}{3(1-r_1)(r_2-r_1)u}\right. \\
& \left. -\frac{1}{2(r_2-r_1)^2(1-u)^2}-\frac{1}{2(r_2-r_1)^2u^2}+\frac{1}{3(\rho-1)^2}\right)G(\rho) \\
& +\left(\frac{1}{3(r_2-r_1)^2u^2}-\frac{1}{3(r_2-r_1)ur_1}+\frac{1}{3(\rho-1)r_1}-\frac{1}{6(\rho-1)^2r_1}\right)\ln(1-r_1) \\
& +\left(\frac{1-2r_2}{6r_2(\rho-1)^2}+\frac{1}{3(r_2-r_1)r_2(1-u)}+\frac{1}{3r_2(\rho-1)}+\frac{1}{3(r_2-r_1)^2(1-u)^2}\right)\ln(1-r_2) \\
& +\left(\frac{r_1+r_2-2}{2(1-r_1)(r_2-1)(\rho-1)}-\frac{1}{2(r_2-r_1)(r_2-1)(1-u)}-\frac{1}{2(1-r_1)(r_2-r_1)u}\right. \\
& \left. -\frac{1}{(\rho-1)^2}-\frac{2}{(\rho-1)^3}\right)\ln\left(\frac{m_b^2}{\mu^2}\right) \\
& -\left(\frac{5r_1+1}{6(1-r_1)r_1(r_2-r_1)u}+\frac{5r_2+1}{6(r_2-1)r_2(r_2-r_1)(1-u)}\right. \\
& +\frac{r_2r_1-4r_1-4r_2+7}{3(1-r_1)(r_2-1)(\rho-1)}-\frac{-2r_2r_1+r_1+r_2}{6r_1r_2\rho} \\
& \left. +\frac{1}{3(r_2-r_1)^2(1-u)^2}+\frac{1}{3(r_2-r_1)^2u^2}+\frac{1}{(\rho-1)^2}\right)\ln(1-\rho) \\
& +\frac{2-r_1-r_2}{6(1-r_1)(r_2-1)(\rho-1)}+\frac{1}{6(r_2-r_1)(r_2-1)(1-u)}+\frac{1}{6(1-r_1)(r_2-r_1)u} \\
& +\frac{5}{3(\rho-1)^2}+\frac{8}{3(\rho-1)^3}\,, \qquad \text{(B.34)}
\end{aligned}
$$

$$
\begin{aligned}
\frac{3}{2\pi}\mathrm{Im}_s T_1^{T\,\sigma} = {} & \theta(1-\rho)\left[\frac{1}{\rho-r_2}\left[\left(-\frac{3}{2(\rho-r_2)}+\frac{1}{r_2-1}\right)L_2(r_2)+\frac{r_2-3}{2r_2(\rho-r_2)}\right]\right.\\
& \left.-\left(\frac{L_2(r_2)}{r_2-1}-\frac{1+L_2(r_2)}{2}\frac{d}{d\rho}\right)\left(\frac{1}{\rho-1}\right)_+\right]\\
& +\theta(\rho-1)\left[\left(\left(\frac{1-L_1(\rho)}{\rho-1}\right)_+ +\frac{1+L_2(r_2)}{2}\left(\frac{1}{\rho-1}\right)_+\right)\frac{d}{d\rho}+\frac{r_1+r_2-2}{(r_1-1)(r_2-1)}\left(\frac{L_1(\rho)}{\rho-1}\right)_+\right.\\
& +\left(-\frac{L_2(r_2)}{r_2-1}+\frac{4-r_1}{r_1-1}+\frac{3}{r_2-1}+\frac{1}{\rho}\right)\left(\frac{1}{\rho-1}\right)_+\\
& +\left(\frac{1}{\rho-r_2}\left(\frac{3}{2(\rho-r_2)}-\frac{1}{r_2-1}\right)+\frac{1}{\rho-r_1}\left(\frac{3}{2(\rho-r_1)}-\frac{1}{r_1-1}\right)\right)L_1(\rho)\\
& +\left(-\frac{3}{2(\rho-r_2)}+\frac{1}{r_2-1}\right)\frac{L_2(r_2)}{\rho-r_2}\\
& -\frac{1}{2}\left(\frac{1+5r_1}{r_1(r_1-1)(\rho-r_1)}+\frac{1+5r_2}{r_2(r_2-1)(\rho-r_2)}-\frac{2}{(\rho-r_1)^2}\right.\\
& \left.\left.-\frac{3(r_2-1)}{r_2(\rho-r_2)^2}+\frac{1}{\rho}\left(\frac{1}{r_1}+\frac{1}{r_2}-2\right)\right)\right]\\
& +\delta(\rho-1)\left[\frac{\pi^2}{4}\left(-\frac{d}{d\rho}+\frac{2}{3}\left(\frac{1}{1-r_1}+\frac{4}{r_2-1}\right)\right)\right.\\
& +\left[\frac{1}{2}\ln^2(1-r_1)+\left(-\ln(r_2-1)+\frac{1}{2}\ln(r_2)+\frac{r_1+r_2-2r_1r_2}{2r_1r_2}\right)\ln(1-r_1)\right.\\
& +\frac{1}{2}\ln^2(r_2-1)-\left(\ln r_2+\frac{1-3r_2}{r_2}\right)\ln(r_2-1)\\
& \left.-3+2\ln\left(\frac{m_b^2}{\mu^2}\right)+\frac{1}{2}\left(\mathrm{Li}_2(r_1)-3\,\mathrm{Li}_2(1-r_2)\right)\right]\frac{d}{d\rho}\\
& +\frac{\ln^2(1-r_1)}{1-r_1}-\left(-2\frac{\ln(r_2-1)}{r_2-1}+\frac{\ln r_2}{r_2-1}+\frac{1}{r_1(1-r_1)}+\frac{1}{r_2(r_2-1)}\right)\ln(1-r_1)\\
& -\left(\frac{2}{r_2-1}+\frac{1}{1-r_1}\right)\ln^2(r_2-1)+\frac{r_1+r_2-2}{2(1-r_1)(r_2-1)}\\
& -2\left(-\frac{2}{r_2-1}+\frac{1}{r_2}+\frac{1}{1-r_1}-\frac{\ln r_2}{r_2-1}\right)\ln\,(r_2-1)\\
& -\left(\frac{3(r_1+r_2-2)}{2(1-r_1)(r_2-1)}+\left(\frac{1}{r_2-1}+\frac{1}{1-r_1}\right)\ln\left(\frac{r_2-1}{1-r_1}\right)\right)\ln\left(\frac{m_b^2}{\mu^2}\right)\\
& +\frac{1}{1-r_1}\left(\mathrm{Li}_2(r_1)-\frac{2r_1+r_2-3}{r_2-1}\mathrm{Li}_2(1-r_2)\right)\\
& \left.-\left(4-3\ln\left(\frac{m_b^2}{\mu^2}\right)\right)\left(\frac{d^2}{d\rho^2}-\delta(r_2-1)\frac{d}{d\rho}\right)\right]\,, \qquad \text{(B.35)}
\end{aligned}
$$

$$\Delta T_1^{T} = -\frac{(\rho+1)\left(3\ln\left(\frac{m_b^2}{\mu^2}\right)-4\right)}{(\rho-1)^2}\,, \tag{B.36}$$

$$\Delta T_1^{T\,p} = 0\,, \tag{B.37}$$

$$\Delta T_1^{T\,\sigma} = \frac{2(\rho+1)\left(3\ln\left(\frac{m_b^2}{\mu^2}\right)-4\right)}{3(\rho-1)^3}\,. \tag{B.38}$$

$$\frac{1}{2\pi}\mathrm{Im}_s\Delta T_1^{T} = \delta(\rho-1)\left(3\ln\left(\frac{m_b^2}{\mu^2}\right)-4\right)\left(\frac{1}{2}+\frac{d}{d\rho}\right)\,, \tag{B.39}$$

$$\frac{3}{2\pi}\mathrm{Im}_s\Delta T_1^{T\,\sigma} = -\delta(\rho-1)\left(3\ln\left(\frac{m_b^2}{\mu^2}\right)-4\right)\left(\frac{d}{d\rho}+\left(\frac{d^2}{d\rho^2}-\delta(r_2-1)\frac{d}{d\rho}\right)\right). \tag{B.40}$$

C. Two-point sum rule for f_B

We use the sum rule with $O(\alpha_s)$ accuracy with the perturbative part calculated in the $\overline{MS}$ scheme for b-quark [18]:

$$f_B^2 = \frac{e^{m_B^2/\overline{M}^2}}{m_B^4}\left[\frac{3m_b^2}{8\pi^2}\int\limits_{m_b^2}^{\overline{s}_0^B} ds e^{-s/\overline{M}^2}\left\{\frac{(s-m_b^2)^2}{s}+\frac{\alpha_s C_F}{\pi}\rho_1(s,m_b^2)\right\}\right.$$
$$+m_b^2 e^{-m_b^2/\overline{M}^2}\left\{-m_b\langle\bar{q}q\rangle\left(1+\frac{\alpha_s C_F}{\pi}\delta_1(\overline{M}^2,m_b^2)+\frac{m_0^2}{2\overline{M}^2}\left(1-\frac{m_b^2}{2\overline{M}^2}\right)\right)\right.$$
$$\left.\left.+\frac{1}{12}\langle\frac{\alpha_s}{\pi}GG\rangle-\frac{16\pi}{27}\frac{\alpha_s\langle\bar{q}q\rangle^2}{\overline{M}^2}\left(1-\frac{m_b^2}{4\overline{M}^2}-\frac{m_b^4}{12\overline{M}^4}\right)\right\}\right]\,, \tag{C.1}$$

where $\overline{M}$ and $\overline{s}_0^B$ are, respectively, the Borel parameter and effective threshold. In the above, the functions determining the spectral density of the $O(\alpha_s)$ corrections to the perturbative and quark condensate terms are

$$\rho_1(s,m_b^2) = \frac{s}{2}(1-x)\Big\{(1-x)\big[4\mathrm{Li}_2(x)+2\ln x\ln(1-x)-(5-2x)\ln(1-x)\big]$$
$$+(1-2x)(3-x)\ln x+3(1-3x)\ln\left(\frac{\mu^2}{m_b^2}\right)+\frac{1}{2}(17-33x)\Big\}, \tag{C.2}$$

where $x=\frac{m_b^2}{s}$, and

$$\delta_1(\overline{M}^2,m_b^2) = -\frac{3}{2}\left[\Gamma\left(0,\frac{m_b^2}{\overline{M}^2}\right)e^{m_b^2/\overline{M}^2}-1-\left(1-\frac{m_b^2}{\overline{M}^2}\right)\left(\ln\left(\frac{\mu^2}{m_b^2}\right)+\frac{4}{3}\right)\right], \tag{C.3}$$

respectively, and $\Gamma(n,z)$ is the incomplete Γ function.

References

[1] I. I. Balitsky, V. M. Braun and A. V. Kolesnichenko, Nucl. Phys. **B312** (1989) 509; V. M. Braun and I. E. Filyanov, Z. Phys. **C44** (1989) 157; V. L. Chernyak and I. R. Zhitnitsky, Nucl. Phys. **B345** (1990) 137.

[2] V. M. Belyaev, A. Khodjamirian and R. Rückl, Z. Phys. C **60** (1993) 349.

[3] V. M. Belyaev, V. M. Braun, A. Khodjamirian and R. Rückl, Phys. Rev. D **51** (1995) 6177.

[4] A. Khodjamirian, R. Rückl, S. Weinzierl and O. I. Yakovlev, Phys. Lett. B **410** (1997) 275.

[5] E. Bagan, P. Ball and V. M. Braun, Phys. Lett. B **417**, 154 (1998).

[6] P. Ball, JHEP **9809**, 005 (1998).

[7] A. Khodjamirian, R. Rückl and C. W. Winhart, Phys. Rev. D **58** (1998) 054013.

[8] A. Khodjamirian, R. Rückl, S. Weinzierl, C. W. Winhart and O. I. Yakovlev, Phys. Rev. D **62**, 114002 (2000).

[9] P. Ball and R. Zwicky, JHEP **0110** (2001) 019.

[10] P. Ball and R. Zwicky, Phys. Rev. D **71** (2005) 014015.

[11] M. A. Shifman, A. I. Vainshtein and V. I. Zakharov, Nucl. Phys. B **147** (1979) 385, 448.

[12] A. Khodjamirian and R. Ruckl, in *Heavy Flavors*, 2nd edition, eds., A.J. Buras and M. Lindner, World Scientific (1998), p. 345, arXiv:hep-ph/9801443.

[13] V. M. Braun, in *Progress in heavy quark physics*, p. 105-118, Rostock (1997), arXiv:hep-ph/9801222.

[14] P. Colangelo and A. Khodjamirian, in *At the frontier of particle physics*, Vol. 3, 1495-1576 ed. by M. Shifman (World Scientific, Singapore, 2001), arXiv:hep-ph/0010175.

[15] A. Khodjamirian, T. Mannel and N. Offen, Phys. Lett. B **620** (2005) 52; Phys. Rev. D **75** (2007) 054013.

[16] F. De Fazio, T. Feldmann and T. Hurth, Nucl. Phys. B **733** (2006) 1; arXiv:0711.3999 [hep-ph].

[17] M. Beneke, G. Buchalla, M. Neubert and C. T. Sachrajda, Phys. Rev. Lett. **83** (1999) 1914; Nucl. Phys. B **606** (2001) 245.

[18] M. Jamin and B. O. Lange, Phys. Rev. D **65**, 056005 (2002).

[19] P. Ball, V. M. Braun and A. Lenz, JHEP **0605** (2006) 004.

[20] I. I. Balitsky and V. M. Braun, Nucl. Phys. B **311** (1989) 541.

[21] T. M. Aliev, H. Koru, A. Ozpineci and M. Savci, Phys. Lett. B **400** (1997) 194.

[22] G. Duplančić, B. Nižić, Eur. Phys. J. C **35** (2004) 105.

[23] G. P. Lepage and S. J. Brodsky, Phys. Lett. B **87**, 359 (1979); Phys. Rev. D **22**, 2157 (1980); A. V. Efremov and A. V. Radyushkin, Phys. Lett. B **94**, 245 (1980); Theor. Math. Phys. **42**, 97 (1980).

[24] T. M. Aliev and V. L. Eletsky, Sov. J. Nucl. Phys. **38** (1983) 936.

[25] A. A. Penin and M. Steinhauser, Phys. Rev. D **65** (2002) 054006.

[26] R. Rückl, S. Weinzierl, O.I. Yakovlev, hep-ph/0007344, hep-ph/0105161.

[27] J. H. Kühn, M. Steinhauser, and C. Sturm, Nucl. Phys. B **778** (2007) 192.

[28] W. M. Yao *et al.* [Particle Data Group], J. Phys. G **33** (2006) 1.

[29] A. Khodjamirian, T. Mannel and M. Melcher, Phys. Rev. D **70** (2004) 094002.

[30] A. P. Bakulev, K. Passek-Kumericki, W. Schroers and N. G. Stefanis, Phys. Rev. D **70** (2004) 033014 [Erratum-ibid. D **70** (2004) 079906].

[31] B. L. Ioffe, Prog. Part. Nucl. Phys. **56** (2006) 232.

[32] M. Jamin, J. A. Oller and A. Pich, Phys. Rev. D **74** (2006) 074009.

[33] V. M. Braun, E. Gardi and S. Gottwald, Nucl. Phys. B **685** (2004) 171.

[34] V. M. Braun and I. E. Filyanov, Z. Phys. C **48**,239 (1990).

[35] B. Aubert *et al.* [BABAR Collaboration], Phys. Rev. Lett. **98** (2007) 091801.

[36] P. Ball, Phys. Lett. B **644** (2007) 38.

[37] D. Becirevic and A. B. Kaidalov, Phys. Lett. B **478** (2000) 417.

[38] E. Barberio *et al.* [HFAG Collaboration], arXiv:0704.3575 [hep-ex].

[39] V. M. Braun, A. Khodjamirian and M. Maul, Phys. Rev. D **61** (2000) 073004.

[40] P. Ball, arXiv:hep-ph/0308249.

[41] M. Okamoto, PoS **LAT2005** (2006) 013 [arXiv:hep-lat/0510113].

[42] E. Dalgic, A. Gray, M. Wingate, C. T. H. Davies, G. P. Lepage and J. Shigemitsu, Phys. Rev. D **73**, 074502 (2006) [Erratum-ibid. D **75**, 119906 (2007)].

[43] M. C. Arnesen, B. Grinstein, I. Z. Rothstein and I. W. Stewart, Phys. Rev. Lett. **95**, 071802 (2005).

[44] T. Becher and R. J. Hill, Phys. Lett. B **633** (2006) 61 .

[45] J. M. Flynn and J. Nieves, Phys. Rev. D **76**, 031302 (2007).

[46] P. Ball, JHEP **9901** (1999) 010.